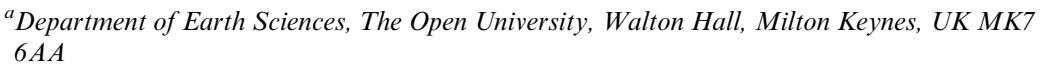
Spectrometry

Update

X-ray fluorescence spectrometry

Philip J. Potts,*a Andrew T. Ellis, Mike Holmes,† Peter Kregsamer, Christina Streli, Margaret West^e and Peter Wobrauschek^d



^bOxford Instruments, Industrial Analysis Group, Wyndyke Furlong, Abingdon, Oxfordshire, UK OX14 1UJ

Received 3rd July 2000 First published as an Advance Article on the web 19th September 2000

- Reviews
- Instrumentation 2
- 2.1 General instrumentation and excitation sources
- 2.2 Detectors
- 3 Spectrum analysis, matrix correction and calibration procedures
- 3.1 Spectrum analysis
- 3.2 Matrix correction and calibration procedures
- X-ray optics
- X-ray optical elements 4.1
- 4.2 Capillary waveguides
- X-ray microfluorescence 4.3
- Synchrotron radiation
- 5.1 Beamlines and optics
- 5.2
- SRXRF instrumentation
- 5.3 **Applications**
- Total reflection XRF spectrometry
- 6.1 Instrumentation and quantification
- Synchrotron radiation-induced TXRF 6.2
- Surface analysis 6.3
- Related techniques 6.4
- **TXRF** Applications 6.5
- Portable and mobile XRF
- 8 On-line XRF
- Applications
- 9.1 Sample preparation
- 9.2 Preconcentration techniques
- 9.3 Geological
- 9.4 Environmental
- Archaeological and forensic 9.5
- 9.6 Industrial
- Clinical and biological 9.7
- 9.8 Thin films
- Chemical state analysis and speciation
- References 10

DOI: 10.1039/b0052841

This annual review of X-ray fluorescence covers developments over the period 1999–2000 in instrumentation and detectors, matrix correction and spectrum analysis software, X-ray optics and microfluorescence, synchrotron XRF, TXRF, portable XRF and on-line applications as assessed from the published literature. The review also includes a survey of applications, covering sample preparation, geological, environmental, archaeological, forensic, biological, clinical, thin films, chemical state and speciation studies. During the current

review period, further advances have taken place in the development of high resolution semiconductor detectors and in the design and application of XRF instrumentation for space and planetary research. Overall, the papers reviewed here again confirm the important contribution the XRF technique makes to a wide range of scientific endeavour.

1 Reviews

It is a pleasure to report another buoyant year in the development of XRF techniques with continued advances in the fields of detector technology, synchrotron beam lines and applications, especially in microfluorescence, PXRF, SR and TXRF. One aspect that was missing was a plethora of fundamental reviews, but Wobrauschek *et al.*¹ did review aspects of X-ray fluorescence analysis and van der Vegt and Norman⁴⁴⁶ took a fresh look at user friendly aspects of WD-XRF. Harada and Sakurai⁴⁴⁷ undertook a review of techniques (including the use of quasimonochromatic excitation using a primary beam filter) for the excitation of K-lines of high Z elements by EDXRF. Finally, Mirenskaya et al.² reviewed the preparation of a series of glassy reference samples designed for the XRF analysis of multicomponent oxide materials, with specific reference to Ti-Ba-Nd-Sm oxides.

2 Instrumentation

2.1 General instrumentation and excitation sources

A novel high-sensitivity XRF analyser for measuring trace elements was constructed by Cheburkin and Shotyk³ using a multi-crystal pyrographite assembly (MPA) to reduce the continuous background and improve detection limits. The MPA functioned as a 'bandpass filter' and was positioned between the sample and Si(Li) detector and adjusted so that only the region of the spectrum containing the Pb lines and a few other trace elements were transmitted. The X-ray lines of other elements as well as coherent and incoherent scatter peaks could not reach the detector owing to incompatible Bragg angles. The authors reported a reduction by a factor of 400 in the intensity of coherent and incoherent scattering from a sample of fossil plant material, with a lower limit of detection (LLD) for Pb of 0.1 $\mu g \ g^{-1}$ in NIST SRM 1515 apple leaves. Considerable improvements were also reported in the LLD for Br and Rb. The MPA may also be adjusted to reduce the continuous background and improve detection limits for elements from Z=22 (Ti) to 39 (Y) (K lines) and from Z = 57 (La) to 92 (U) (L lines).

Further work was published on the development of analysing

^cCeram Research, Queens Road, Penkhull, Stoke-on-Trent, UK ST4 7LQ

^dAtominstitut der Österreichischen Universitäten, Stadionallee 2, A-1020 Vienna, Austria

^eMaterials Research Institute, Sheffield Hallam University, City Campus, Howard Street, Sheffield, UK S1 1WB

[†]Review co-ordinator to whom correspondence should be addressed and from whom reprints may be obtained.

[†]Present address: 19 Denstone Crescent, Blurton, Stoke-on-Trent, Staffs, UK ST3 4BX.

crystals. Hombourger et al.4 used layered synthetic microstructures (LSM) for measurements of selected long wavelength X-rays. The lines, C Kα and N Kα, were studied with W/ Si (d=3.25 nm), whilst Ni/C (d=4.8 nm) was found to be better than Mo/Si (d = 5.0 nm) or B/Si (d = 4.6 nm) for B Ka. A new spectroscopic technique using thin crystals was described by Ogata and Kitamoto,⁵ who demonstrated the capabilities of this instrument by clearly resolving the Ti $K\alpha_1$ and Ti $K\alpha_2$ lines. The design of a multi-crystal X-ray spectrometer and its applications in the fields of XRF and X-ray Raman spectroscopy was described by Bergmann and Cramer⁶ of the Lawrence Berkeley National Laboratory in California. Based on 8 spherically curved Si crystals bent to a radius of 86 cm, the crystals were individually aligned in the Rowland geometry to capture a solid angle of 0.07 sr. Energy scans were obtained by moving the whole instrument rather than scanning each crystal by itself. Although designed for X-ray absorption and fluorescence spectroscopy of transition metals in dilute systems such as metalloproteins, the instrument may also be used for Xray Raman spectroscopy studies.

Experimental studies contributing to the *development of instrumentation* for imaging by means of characteristic X-rays were published by Baskaran and Selvakumaran⁷ who described a compact electron cyclotron resonance (ECR) plasma X-ray source. This configuration has a potential use for medical imaging. Ullmann *et al.* 8 measured ion charge state distribution (CSD) in ECR plasma X-rays to contribute to a better understanding of the influence of microwave power, magnetic field, neutral gas pressure and gas mixture on the plasma and to improve source operation.

A multilayer grating spectrometer for solar observations was described by Antonucci et al.⁹ at the 1998 meeting of SPIE—The International Society for Optical Engineering. Andrus and Powell¹⁰ also presented a paper on soft X-ray filters designed for transmission between 40 Å and 170 Å for use in solar astronomy. Single foils and multilayer combinations of Nb, Pd, Rh and Zr were fabricated with polyamide as a support film.

A novel crystal X-ray generator using small pyroelectric crystals, such as LiTaO₃, surrounded by gas at pressures of 15 mT was described by Shafroth and Brownridge. ¹¹ When one surface of the crystal was heated, a strong electric field was produced at the opposite side of the crystal and electrons accelerated towards it generating Ta L and M radiation. On cooling, the direction of the electric field was reversed and a target X-ray spectrum was obtained. The instrument was designed for student experiments to demonstrate various properties of X-rays.

Developments of other X-ray excitation sources were published by Bassari and Gencay. The radioisotope 99mTc was added to samples in experiments to study the possibility of using the emissions from this source to excite fluorescence in the sample. The activity necessary to achieve optimum accuracy was reported. Yajima et al. 13 proposed a simple method to produce quasi-monochromatic X-rays by photoabsorption-edge transition radiation tuned by tilting a stack of either titanium foil or a Kapton foil and titanium filter combination.

Other instrumental developments included an EDXRS study by Tartari et al. 14 of a new collimator for enhanced scattering techniques. A 90° scattering geometry was considered in order to maximize the spatial resolution by using two parallel plates perpendicular to both the detector surface and the plane of first scattering. Enhancement of the main Compton and coherent peaks was reported when compared with the classical highly collimated geometry. Schramm et al. 15 reported a fast screening method for qualitative or semi-quantitative analysis using polarized X-rays. Uhlig et al. 16 introduced a new 1 kW WDXRF spectrometer system requiring mains power and no external cooling water nor detector gas. The configuration was reported to have the full analytical performance of traditional

3-4 kW systems. An eight channel X-ray spectrometer for the 0.2–1.5 keV energy range was developed by Bessarab et al. 1 Each channel had a calibrated band pass consisting of filter, multilayer mirror and vacuum X-ray diode. Tolokonnikov¹⁸ described a secondary target system for simultaneous analysis of powder and liquid samples of up to 25 elements ranging from Ca to U. Elemental quantification using multiple-energy X-ray absorptiometry was reported by Kozul et al. 19 for Al and Zr foils and these workers also reported X-ray microtomographic measurements of solid samples and aqueous solutions. A long-term statistical study of the stability of two X-ray spectrometers over an extended period of ten years was reported by Dlouhy et al.20 as part of a QA/QC programme. Conclusions were made about the different methods for limiting the effect of fluctuations in spectrometer response by using monitor ratio or performing a new calibration.

Patent claims for innovations in XRF this year included Schimizu²¹ for an X-ray spectrometer for elemental and structure analysis, based on secondary target excitation. A sample mask and holder were described by Makiishi et al.²² for the analysis of rapidly cooled metal slugs, which had been rapidly solidified from the molten state by spreading over a 'trigonal' column or flat plate. Tsuruya et al. 23,24 offered a device for the accurate determination of S in a flow sample, incorporating a beryllium foil of improved corrosion resistance. Kono and Kuraoka²⁵ claimed a device for the rapid compensation of the analytical error due to variation of the distance between sample and radiation source or due to change in vacuum conditions. Ma²⁶ described a method and hardware for the measurement of metallic impurities in a fluid by XRF in which a sample stream was passed at constant flow rate through a microporous filter. Finally, Kuwata and Saito² described a spectrometer incorporating two X-ray tubes designed to prevent high voltage power breakdown by ensuring little fluctuation in the load from the power source.

2.2 Detectors

Very high-resolution cryogenic energy dispersive detectors remained, as was the case for last year's update, the headline interest, notwithstanding further developments in silicon drift detectors discussed later in this section. However, in the area of high-resolution cryogenic detectors, Stahle and colleagues²⁸ at NASA reviewed microcalorimeters with particular reference to their use in space for X-ray astronomy. The limitations of doped semiconductor materials used in microcalorimeters were reviewed by McCammon and co-workers.²⁹ These authors discussed the potential for further improvement, including aspects of detector design in this important class of ED detector. Hoehne and co-workers^{30,31} at TU Munich reviewed the group's work in developing microcalorimeter and, more recently, superconducting tunnel junction (STJ) high-resolution ED detectors. Both types of detector are being studied by the group for their use in scanning electron microanalysis and in the more exotic areas of high-energy physics experiments and astrophysics.

In a further contribution, Hoehne and colleagues³² described in detail the realization of a *microcalorimeter* based upon an indium–gold phase transition thermometer. The initial results were reported at the European EDXRS conference in Bologna during June 1998 and in the 1998 Analytical Spectrometry Update, but the full paper has a well presented description of the detector and its key design and operational characteristics. The device itself was a 250 × 250 µm gold absorber with 50% efficiency at 5.9 keV which, when operated at 30 mK, yielded an impressive energy resolution of 15.5 eV at 5.9 keV, although at a low input count rate of only 50 cps. A patent³³ for this type of microcalorimeter was published and an instrument based on this design is now commercially available. Adams and coworkers³⁴ described a magnetic microcalorimeter based on

600 μg g⁻¹ paramagnetic Er³⁺ ions embedded in gold, which was designed for the detection of X-rays with energy up to 100 keV. When operated at 55 mK the device was reported to yield an energy resolution of 90 eV at 5.9 keV, although the authors predicted that further optimization would deliver <2 eV energy resolution at 50 mK. Holland and colleagues³⁵ at Leicester University, UK, described their work on Al-Ag transition edge calorimeters and indicated that the goal of 2 eV energy resolution at 1 keV may well be achievable. The authors described some of the technological challenges presented by these devices, which limit their reliability and longevity. Seemingly undeterred by the awesome technological challenge posed by these cryogenic microcalorimeters, scientists in the US and Japan collaborated, not only to develop a 32-element array of microcalorimeters, but then to fly the resulting XRS Xray detection system on the ASTRO-E astronomy satellite. Mitsuda and Kelly³⁶ described work based at the NASA Goddard Space Flight Center on their novel 3-stage cryogenic system comprising solid neon, liquid helium and an adiabatic demagnetization refrigerator. The lifetime of this detection system was set by the slow loss by evaporation of the solid neon, which was expected to be around 2 years. Breon et al., 37 at NASA, reported the initial development and assembly of the cryogenic system whilst Stahle *et al.* ³⁸ described in detail the design and optimization of the microcalorimeter system itself. The 32-element detector array comprised ion-implanted thermistors and HgTe X-ray absorbers and delivered an impressive energy resolution of 9 eV at 3 keV and 11 eV at 5.9 keV. Audley et al. 39 described the calibration of the XRS detector system and the nature of the platinum X-ray mirror used to focus X-rays onto the 32-element microcalorimeter detector array. The authors described the methods used to determine the X-ray spectral characteristics and efficiency across all the detectors in the array. The XRS detection system is very impressive and once more underlines the importance of space missions and X-ray astronomy in raising the profile of new X-ray detection technologies that will, one day not so far away, become much more common in terrestrial X-ray fluorescence analysis.

Kurakado,40 who has been involved in superconducting tunnel junction (STJ) detectors from the outset, presented a comprehensive review of the main operating principles and development of this important emerging class of very high resolution energy dispersive X-ray detectors. The author presented the state of the art, which at that time was < 30 eV energy resolution at 5.9 keV and 6 eV at 277 eV with operating count rates of more than 10 kcps. Hettl and colleagues⁴¹ reported an impressive energy resolution of 12 eV at 5.9 keV from a 100 μ m \times 100 μ m Al-Al_xO_y-Al STJ detector. The incident radiation was carefully confined to the detector itself, which minimized noise from the detector leads and substrate, yielding an electronic noise of 7 eV. Friedrich et al. 42 reported a similar energy resolution of around 10 eV at 10 kcps, but carried out further development to produce an array of STJs. This array retained the impressive energy resolution of a single STJ but offered much higher total count rates as each element in the array retained its ability to contribute a count rate of 10 kcps. A further report from this $group^{43}$ described the development of Nb-Al-Al_xO_y-Al-Nb STJs which, when operated below 400 mK, provided energy resolution of 8.9 eV at 1 keV. The authors used the detector for high resolution L-edge X-ray absorption spectroscopy of dilute metalloprotein samples. Kraft et al. 44 reported their work on the development of STJ detectors at the European Space Agency. The interest of this group was in the use of the detectors for astronomy and the devices were characterized over a wide energy range from near-IR, through visible and UV, to medium X-ray energies (2-10 keV). The authors described the initial performance of a 6×6 array of STJs and in this and a further publication⁴⁵ reported some of the

mechanisms affecting energy resolution and aspects of the models used to describe the photo-absorption and tunnelling effects in STJs. Finally, Adrianov and co-workers⁴⁶ discussed some of the back-tunnelling and phonon effects that they had observed in Nb–Al–Al_xO_v–Al–Nb STJ X-ray detectors.

The excitement at the cutting edge of X-ray detectors may appear to have been centred on microcalorimeters and STJs, but the review period has also seen a considerable volume of interest in silicon-based semiconductor detectors. Of particular interest in this very important area has been the further development of silicon drift detectors (SDD). Castoldi and coworkers⁴⁷ at Politecnico di Milano, Italy, provided a timely and authoritative review of SDD in which they described the basic principles and designs used. More-recent advances in the area of the new and novel pixellated controlled drift detector were described. Two-dimensional, position-sensitive data were obtained whilst retaining the key performance indicators of high energy resolution for this type of device (205 eV at 5.9 keV) and high count rate (>10 kcps), even when operated at room temperature. Further details of the design and characterization of this novel new detector were provided in other publications by Castoldi et al. 48-50 A novel design of SDD comprising a continuous implanted drift cathode acting as a high voltage divider was described by Bonvicini et al. 51 The detector had a very large active area of $2 \times 130 \text{ mm}^2$ and the absence of a metallized contact on the front sensitive surface was expected to offer substantial benefits for soft X-ray detection. Iwanczyk and co-workers⁵² also reported their fabrication and characterization of large area SDDs, comprising 8 and 12-mm diameter hexagons fabricated on 350-µm thick high resistivity silicon. The resulting SDDs were tested at -75 °C using an amplifier shaping time of 6 μ s and the resulting energy resolution at 5.9 keV was 159 eV for 5 mm² and 263 eV for 10 mm² detectors. Finally, a new and novel VLSI multichannel shaper amplifier suitable for multi-anode SDDs or other multi-element solid state silicon detectors was described by Fiorini et al. 53,54

The application of *silicon PIN diodes* to XRF analysis is now widespread and there is wide commercial availability, which has led them to be applied elsewhere during the review period. Al-Turany, Meyer and Bethge⁵⁵ applied the Amptek XR-100 CR to PIXE measurements and, during their characterization, found that one of the main features of the detector response model that they derived was the presence of a relatively thick front surface silicon dead layer. Sato⁵⁶ reported the use of silicon PIN diodes for SR-XAFS measurements, whilst Ota *et al.*⁵⁷ assessed them for use in X-ray astronomy. Golubev and co-workers⁵⁸ characterized a number of commercially available devices for use in their X-ray plasma diagnostic studies.

The search for improvements in non-cryogenic cooling systems for practical silicon-based X-ray detectors continued during the review period. Iwanczyk and Patt⁵⁹ reviewed the state of the art for miniaturized solid state X-ray detectors destined for in-vivo XRF instrumentation. Of particular interest to these authors was the design of simple and compact non-cryogenic cooling systems and detector HV bias systems. Struder and colleagues⁶⁰ at TU Munich reported their characterization of SDDs at room temperature and at $-10\,^{\circ}\text{C},$ and also of large area (36 cm²) CCD X-ray detectors operated at -70 °C and destined for use in an X-ray satellite mission. Highly compact and portable XRF systems for the non-destructive analysis of often large works of art and archaeological specimens were the subject of a comprehensive paper by Cesareo and colleagues. 61 The authors described systems based upon silicon PIN, SDD, CdZnTe and HgI₂ detectors, for which the energy resolution at 5.9 keV was 200-300 eV, 155 eV, 300 eV and 200 eV, respectively. In conjunction with an optimal X-ray tube excitation system, these systems provided very effective portable EDXRF systems and their use for a variety of interesting applications was described.

Last, but by no means least, was the impressive thermoelectrically cooled Si(Li) detector reported by Barkan, Ihrig and Abott. ⁶² This was a second-generation Peltier-cooled unit and its performance in terms of energy resolution was shown to be very nearly as good as a conventional, cryogenically cooled, Si(Li) detectors. The performance of the unit tested was claimed not to degrade over a period of several years of use.

Notwithstanding this increasing use of SDD and silicon PIN detectors, particularly in compact EDXRF instrumentation, the Si(Li) detector remains important and continues to be subjected to intense scrutiny in order to better characterize and understand it. Statham⁶³ alluded to a convergence in Si(Li) detector technologies as a result of commercial competition, but cautioned against an assumption that all such detectors were equal in their detailed performance characteristics. Lepy and coworkers⁶⁴ continued their careful studies of detector response and used tuneable monochromatized SR to further develop their Si(Li) and HPGe detector response models in the 1-10 keV energy range. The basic peak model used was a modified Hypermet function but, using their highly versatile source, the authors were able to characterize a strong enhancement in the peak tail above the binding energy for each detector material. The principal physical effects contributing to low energy peak shapes, tailing and background in Si(Li) and HPGe detectors was also the subject of a comprehensive paper by Lowe. 65 One particularly notable feature of this study was the large number of detectors available to the author. Other studies in this area included work by Scholze $et~al.^{66}$ on the electron-hole pair creation energy, Budak $et~al.^{67}$ who measured Si(Li) detector efficiency over the energy range 5.5-60 keV, and Perotti and Fiorini,68 who investigated the variation in Fano factor in silicon over the energy range 5.9-122 keV using an SDD. Of particular note in the latter study was the fact that the change in Fano factor was greater at room temperature than at -35 °C. In their study of escape peaks in Si(Li) and silicon PIN diode X-ray detectors, Karydas and Paradellis⁶⁹ recognized the magnitude and need for correction of rear-side escape in the thinner (300 µm) silicon PIN diode type of detector. A 2-fold reduction in incomplete charge collection background in Si(Li) detectors was reported by Walton and colleagues, 70 using an aluminiumamorphous silicon contact in place of the conventional gold Schottky contact.

Pixellated semiconductor energy dispersive X-ray detectors continue to generate interest for use in applications where either large area and high count rate performance or energy dispersive X-ray imaging was required. Ludewigt and co-workers^{71,72} at LBNL, Berkeley, California, described a 32element silicon detector array for high count rate, low noise Xray spectroscopy. The 32-detector array outputs were individually wire-bonded out to integrated circuits that featured discrete charge sensitive preamplifiers and pulse shaping amplifiers. The signals were then taken off-chip to commercially available storage and display units. Seller and colleaat the Rutherford Appleton Laboratory, Oxford, UK, described their approaches to fully integrated pixellated silicon detector systems in which one embodiment had the detector arrays directly bump bonded to a pulse shaping ADC and readout chip. Rossi *et al.*⁷⁴ developed and characterized a germanium strip detector and a split charge correction procedure that yielded artefact-free spectra but with a dismal energy resolution of slightly better than 2 keV and claimed peak-to-valley ratios of > 1000. A rather more impressive energy resolution of 170 eV at 5.9 keV was claimed by Derbyshire and co-workers⁷⁵ for a 3×3 array of germanium detectors.

The development of *CCD X-ray detectors* continues to be driven principally by their use for X-ray astronomy. Keay and co-workers⁷⁶ reviewed the current state of the art and a team at Hamamatsu⁷⁷ reported their development of a $2k \times 4k$ pixel detector. A report of the fabrication and characterization of an

immensely impressive very large area $(6 \times 6 \text{ cm}^2)$ CCD was presented by Sotau *et al.*⁷⁸ The detector was fully depleted over the whole wafer thickness of 300 μ m, compared to the usual few tens of μ m in previous CCDs, yielding a high detection efficiency over the 0.2–15 keV energy range. Seven high quality devices, at an impressive, but still expensive, production yield of 27% when operated at < 180 K, delivered a uniform spectral response and an extremely impressive energy resolution of 130 eV at 5.9 keV. Three of these detectors have now been incorporated into the cameras due to fly on two satellite missions.

In the area of compound semiconductor X-ray detectors CdTe and CdZnTe (CZT) remain the most studied and most practical and widely used materials, albeit mostly for very high energy Xray or gamma ray detection. Fougeres and colleagues⁷⁹ reviewed the physical and detector characteristics of both CdTe and CZT detectors and concluded that it remained very difficult to choose between these two types of detector. Bale et al.80 coupled a CZT detector to a low noise Pentafet preamplifier and used thermoelectric cooling to between -30and -40 °C, which resulted in a detector with a creditable energy resolution of < 280 eV at 5.9 keV and a PBR > 200:1. Although far from the current performance of Si(Li), SDD or silicon PIN detectors, there is interest in these devices particularly for their much greater stopping power for highenergy X-ray spectrometry and astronomy. These workers and Stahle et al.81 at NASA are fabricating and characterizing CdTe and CZT detector arrays destined for use in hard X-ray and gamma ray astronomy. Finally, Shor, Eisen and Mardor^{82,83} showed substantial reduction of the incomplete charge collection tailing in CZT detectors through the use of a novel method of controlling electron trapping.

The group at Coimbra, Portugal, remained active in their study of *gas proportional scintillation counters* (*GPSC*) during the review period. Dias⁸⁴ described how the Monte Carlo (MC) simulation of xenon gas fill in proportional gas counters led to a better understanding of some experimentally determined discontinuities. Santos *et al.*⁸⁵ and Dias *et al.*⁸⁶ extended the MC simulation work to xenon–neon gas mixtures in GPSCs and calculated values of the Fano factor and mean energy for primary electron production for nine xenon–neon mixtures in the range 5–100% xenon. Silva and Conde⁸⁷ described in detail an improved large area GPSC system with lower volume and mass, which made it more suitable than its predecessors for use in balloon-borne solar X-ray studies. The energy resolution of the resulting system was 4.7% at 22.1 keV and 3.7% at 59.6 keV.

3 Spectrum analysis, matrix correction and calibration procedures

3.1 Spectrum analysis

There were few reports during the review year devoted uniquely to this topic. This is, in part, a result of the application of methods, such as those employing chemometric techniques, in which spectrum analysis and analyte concentration evaluation are combined. Such methods are covered in the following section. Readers are also referred to Section 2.2 on detectors, in which there is coverage of reports on detector characterization, especially peak shape models, which are important for successful peak area estimation in EDXRF spectrometry.

The challenge of *peak deconvolution of proportional counter* spectra obtained from geological materials excited with a radioisotope source was addressed by Boyle. The author described the problems associated with using pure element spectra for the evaluation of overlap factors and derived a detector peak model that could be used. In addition to the basic photopeak shape that was readily represented using a Gaussian with an exponential tail, the model included corrections for dead time, sum peaks, escape peaks and tailing due to wall

effects. The width of the exponential tail was established empirically from measurements on pure element samples to be 7.3 keV for all peaks. Surprisingly, sum peaks were reported to be found not at $2 \times$ the parent peak energy but at $1.95 \times$ that energy. Peak shift at high count rates was not included in the model, but all measurements were carried out at a rate low enough to avoid significant peak shift. The new model was successfully applied to the determination of 15 minor and trace elements in geological samples, yielding some impressively low calibration uncertainties and detection limit values. In a separate study on geological samples, Long *et al.* ⁸⁹ dispensed with any type of peak modelling and applied an artificial neural network technique with satisfactory results using both X-ray tube and radioisotope excitation.

The strongly overlapping S K and Pb M series lines in EDXRF spectra were the subject of a detailed study by Facchin et al. 90 into the use of chemometric techniques. The four chemometric techniques employed included three partial least squares (PLS) variants and one based on an artificial neural network (ANN). These methods were compared to the commonly used Lucas-Tooth and Price (LTP) intensity correction model, which was in this case based only on peak height. The calibration/training set comprised 38 synthetic samples prepared from charcoal and containing sulfur and lead over the concentration range 2–17% m/m. Commercially available standard software packages were used for all methods and the ANN system comprised an input and an output layer with one hidden layer. The ANN method yielded the best standard error of prediction of 4% m/m for S compared to those from polynomial PLS, linear PLS and LTP of 8.6, 7.8 and 8.3% m/m S, respectively. In the case of Pb, the standard error of prediction for ANN was 9.2% Pb compared with 13.3, 17.2 and 10.2% m/m Pb for the other methods, indicating that there was little to be gained over a straightforward (LTP) intensity correction model. This probably reflects the poor quality of the raw Pb L series data, excited as they were with an X-ray tube potential of only 15 kV, which leads to very poor signal to background ratios and the inevitably poor final results. In a tube-excited EDXRF system, there is ample opportunity to improve this situation. This was an interesting piece of work, but it acts as a timely reminder that a high quality initial spectrum is a far more important step in getting high quality reliable data than the application of any number of novel mathematical procedures.

Bao⁹¹ proposed a correction that combined measured background, overlaps and matrix correction. The method was applied to the determination of Mo in light geological matrices, using the Rh Ka Compton backscattered radiation to correct for the background of the analyte Mo K line. The first and second order overlaps from Zr K and Sr K, respectively, were also incorporated. Using the Rh K Compton for the background correction yielded a standard error of 3.3 $\mu g \ g^{-1}$ Mo based on data from 26 calibration samples covering the concentration range $0.3-92 \mu g g^{-1}$ Mo. The author commented that the method could only be applied to samples with a light matrix and a limited composition range. The inclusion of the first order overlap using the Zr $K\alpha$ line improved the standard error to $0.66 \,\mu g \, g^{-1}$ Mo and further inclusion of the second order overlap using Sr Ka data give a further improvement to $0.42 \mu g g^{-1}$. These data clearly demonstrate the importance of including effective background and full overlap corrections. The method, as for all corrections using Compton peaks, required the absence of major and minor element edges in the analytical region of interest and that the Compton peak properly represented the background under analyte and all overlapping lines.

3.2 Matrix correction and calibration procedures

As indicated in the spectral analysis section above, interest continued during the review period into the application of

chemometric techniques to EDXRF analysis. Lemberge and Van Espen⁹² used PLS regression to determine As, Cu and Ni in aqueous solutions from the hydro-metallurgical industry. The concentration of the analytes was in the range 0.5–50 g l^{-1} . The benefits claimed for the method were its ability to combine in a single fast step both the spectrum processing and quantification process, and the avoidance of specific analytic models for peak shape or quantitative calibration. Of the 22 samples used in the study, 10 were used for the calibration training set and 12 for checking accuracy of prediction. Four different methods of pre-processing the spectra prior to their being passed to the PLS regression procedure were investigated. The logarithm pre-processing procedure resulted in a standard error of prediction twice as great as the other procedures based on direct raw data or square root processing and was excluded from further study. For all the PLS procedures, the typical optimum number of latent variables was found to be 3. Overall, the best values of standard error of prediction were obtained with either no spectrum pre-processing or pre-processing using a square root function. The top hat filter, which is widely used for suppressing continuum background in EDXRF spectrum processing, showed no benefit over the other pre-processing methods studied. The finally selected PLS regression was found to be comparable to the widely used Lucas-Tooth and Price (LTP) intensity correction procedure, which used net intensities generated by the AXIL non-linear least squares spectrum fitting program. The benefit of the PLS approach lay principally in its single step processing, although with such simple spectra it would be interesting to see how well the LTP model would function using simple gross peak intensities and a Compton peak correction, which would also be a single step rapid process.

The review period was also less active in the area of fundamental parameter (FP) calculation methods than in previous years. However, the details of an FP analysis program VERBA-XRF were described by Verkhovodov, 93 who claimed that accuracy was good enough for the routine determination of up to 50 elements, even in the presence of undetectable elements such as B, C, N and O. Simakov and Isaev⁹⁴ found their FP method to be as accurate as one based on a new mathematical model that the authors had derived for estimating mass absorption coefficients in an unknown matrix, providing an internal standard was used. The methods were validated for the determination of V in rare earth reference materials to which Zr was added as internal standard element. Weber et al. 95 applied an FP procedure to the interesting analysis of carbon grids on metallic substrates. The study revealed that the C Ka line intensity was enhanced as the energy of the incident primary radiation increased and this effect was attributed by the authors to be due primarily to excitation by photoelectrons generated after the initial primary excitation. A theoretical model was derived for this effect and good agreement was found for higher exciting voltages, although deviations of up to 20% were found for lower excitation voltages.

The important area of *characterizing X-ray tube spectra* remained active during the review period. Ebel, ⁹⁶ who has made a significant contribution to this area of knowledge in the past decade, provided a comprehensive review of the subject. The more recent work by Ebel and colleagues at TU Vienna was described in detail and shown to be widely applicable, and generally more accurate, than that of the then NBS during the 1980s. Use of the NBS algorithm should, according to Ebel, be restricted to electron incidence angles close to 90 degrees and to the higher range of applied X-ray tube kV. Broll and de Chateaubourg ⁹⁷ presented spectral data for end window X-ray tubes equipped with gold, rhodium, chromium or copper targets measured directly using an ED method. The measured continuum was compared to that calculated using a semiempirical expression based on the well-known Kramers

equation. The measured characteristic line spectrum relative intensities were calculated but not mathematically modelled. Although limited to the simulation of ED spectra arising from electron excitation in an SEM, an algorithm developed by Acosta *et al.* ⁹⁸ may be extendable to generate X-ray tube spectra as it provided good agreement with experimental data for samples of stainless steel, bulk chromium and bulk copper.

Conventional matrix correction procedures remain the mainstay of routine XRF analysis and improvements to them continue to be made. Lachance⁹⁹ has been involved in developing influence coefficient methods for very many years and provided a valuable review of their merits and important inter-relationships. The author observed that there has been heated discussion over the years as to the validity and applicability of the variously proposed models and the associated influence coefficients. Lachance asserted that all validly derived algorithms were equivalent in representing the XRF emission process, but some are expressed in models that are more convenient to apply. Conversely, influence coefficients are usually defined for specific analysis contexts but theoretically based coefficients should be as equivalent as the models in which they are used. The author concluded by suggesting that no theoretically derived model or its coefficients should be regarded as pre-eminent and that advances in any one should be capable of being applied to all others. As if to mirror this view, Cloete¹⁰⁰ compared a number of software packages for their use in the analysis of silicates as fused disks. The magnitude and sign of the coefficients were compared and only minor differences in analysis accuracy were found for a variety of geological samples. A comparison of the LTP, Raspberry Heinrich and de Jongh correction algorithms was reported, 101 unsurprisingly, to yield significant improvements in analytical accuracy after application of the LTP correction to the analysis of phosphate minerals and soil samples. Pavlinsky and Vladimirova¹⁰² derived a new model that was a practical approximation of Sherman's FP equations. The authors investigated in detail the enhancement and third-element effects using as an example the data quoted in the classic Raspberry-Heinrich paper on the Cr-Fe-Ni ternary system. The effect of composition change on the coefficients representing enhancement was carefully evaluated and the best formalism yielded improvements in the results from the model of $11.6 \times , 6.2 \times$ and $23 \times$ for Cr, Fe and Ni, respectively. Accuracy using the new model was compared to that obtained from both the Raspberry-Heinrich and the Broll correction models. The newly proposed model gave exceptionally good accuracy for the high alloy steels to which it was applied and was considered not to need concentration-dependent influence coefficients. Finally, in a paper dealing with semi-quantitative analysis, Garcia and Figueroa¹⁰³ described a method in which simple peak areas were plotted on a polygonal graphic representation. Using known materials and selected elements, clusters of similar composition type could be used to identify unknown soil and plant material according to an empirical correlation factor. Such a simple approach is of very limited use when straightforward wide range calibrations for these types of materials or FP calculations are well suited to delivering reliable quantitative analysis.

The use of scattered radiation for matrix correction in a wide variety of sample types and compositions continued to generate interest during the review period. Vincze and colleagues¹⁰⁴ extended their Monte Carlo (MC) simulation of XRF spectra to the study of photon scattering at high X-ray energies (60–100 keV). The simulation data showed good agreement with those measured from aluminium, copper and polypropylene samples excited using monochromatic SR and an HPGe detector at the Hasylab SR facility. Multiple Compton and Rayleigh scattering was readily observed from the light matrices of polypropylene and aluminium and these effects were modelled successfully by the authors' MC code. In the

first paper of a series on uncertainty in quantitative XRF analysis, Rashmi and Suri¹⁰⁵ addressed the widely used Compton scatter method. All sources of uncertainty were established for the case of a heavy element (iron) in a light matrix (silicon). The authors provided a useful and detailed appendix of the equations used. In two Chinese language publications, Bao et al. 106,107 reported details of the relationship between Compton and continuum backscatter radiation and the sample mass absorption coefficient. In both cases, the usual assumption of inverse proportionality was found to be substantially less accurate than a power function. In the case of the continuum scatter at 0.081 nm (15.3 keV), the 1.22 power function yielded a 4-fold improvement in accuracy over the standard inverse Compton method for the determination of Sr in a variety of geological samples. In an important and interesting contribution, Duvauchelle $et\ al.^{108}$ reported a new method for calculating the effective atomic number of a sample from the Compton to Rayleigh (C:R) scattering ratio. It was found possible to adjust experimental conditions to obtain a C:R ratio that was almost independent of X-ray attenuation inside the sample. The authors used monochromatic excitation from a ²⁴¹Am radioisotope source and a germanium ED X-ray detector to ensure adequate Compton-Rayleigh peak separation. A useful review of the C-R method and the various methods for calculating effective atomic number was presented and a new approach to calculating effective atomic number was proposed. Although more complex than earlier methods, the new method offered a wide range of application and was claimed to be a more logical way to represent the physical effects that are at work in producing this very useful relationship. Finally, Kuczumow et al. 109 described how the Compton and Rayleigh scattered peaks and the transmitted Xray signal could be used to establish the density of samples whose density varied periodically through the bulk. The theoretical basis of the generation of these signals was presented and the method was used for XRMF analysis of samples such as wood sections or stalactites with naturally periodic structures. The paper showed that the use of Compton and Rayleigh signals in XRMF could replace the need for Xray transmission measurements in that technique. The combination of the Compton-Rayleigh density measurements with those of the elemental fluorescence X-ray signals can give much richer information in this increasingly important area of XRMF analysis.

4 X-ray optics

X-ray optical elements are generally used to focus or collimate primary X-ray beams for X-ray microfluorescence (XRMF) applications. In this section, general aspects of the topic are reviewed. More specialized aspects associated with synchrotron radiation (SR) applications are reviewed in Section 5.

4.1 X-ray optical elements

Several *reviews* considered a range of topics relevant to X-ray optical elements. Willingale¹¹⁰ considered the basic physics of the interaction between X-rays and matter and the role of mirrors, multilayers, crystals and gratings. Geometries used for X-ray imaging and spectroscopy, with particular reference to X-ray astronomy applications, were also described. Adams *et al.*¹¹¹ reviewed the current state of atomic resolution X-ray holography. Hudec *et al.*¹¹² outlined the basic ideas and approaches to the replication of X-ray optics as an alternative to the direct polishing of grazing incidence mirrors. Aristov¹¹³ reviewed the fabrication of Bragg–Fresnel optics, and applications including X-ray scanning microscopy and X-ray lithography.

Multilayers are widely used as focusing elements in X-ray optics and the design and performance of laterally graded

multilayer X-ray mirrors based on sputter deposition techniques was discussed by Morawe et al. 114 Multilayer coated gratings for high energy (>6 keV) X-ray spectroscopy applications were discussed by Tamura et al., 115 who presented results of experimental measurements of the efficiency and resolution of a Pt-C multilayer. Kozhevnikov et al. 116 studied theoretical aspects of multilayer X-ray mirrors with a wide spectral band of reflection, achieved using depth-graded multilayer coatings. Their work involved developing a computer model for simulating the spectral dependence of reflectivity over a wide spectral range for a defined multilayer d-spacing profile. The use of Kirkpatrick-Baez multilayer optics for XRF imaging of a specimen under X-ray illumination was described by Bakulin *et al.*¹¹⁷ Multilayer optical elements were placed close to the specimen to form a magnified image at an area detector positioned about 0.5 m away from the source. Recent advances in the field of soft X-ray etched multilayer optics were described by Wang et al., 118 based on the

fabrication of Mo–Si multilayers by magnetron sputtering. A series of papers from Japanese collaborators ^{119–122} described the *manufacture of large reflection mirrors* that had both an extremely high surface finish and high form accuracy. CVD-SiC is a promising material due to its unique properties, but is not widely used because of its poor machinability. The authors described the process of ELID (electrolytic in-process dressing) lap grinding as an ultra-precision polishing method to form aspherical and flat mirrors.

In terms of *instrumental developments*, Ohara¹²³ developed low energy X-ray optics which increased the solid angle of fluorescence X-rays 'seen' by a standard ED detector to compensate for the finite sample–detector distance found in conventional EDXRF systems. This development was claimed to be able to increase the detected count rate for B K α by a factor of 22 times.

4.2 Capillary waveguides

Innovations continue in the use of capillary collimators for XRF microprobe analysis, with particular interest in polycapillary collimators (also known as the Kumakhov lens). Bzhaumikhov et al. 124 described a new method of microanalysis using instrumentation in which a polycapillary conic structure was used for the collimation of fluorescence radiation emitted by the sample. Using this device, the primary beam could be used to excite a large area on the sample with the detected fluorescence spectrum restricted to a surface area of down to 20 µm by the polycapillary collimator. Nikitina et al. 125 described the performance of a polycapillary collimator in a more conventional configuration in which the collimator was placed in front of the X-ray tube to increase the intensity of primary radiation exciting a selected area on the sample by at least two orders of magnitude. Using this configuration, detection limits of 0.1 pg could be achieved using a low power (2 W) X-ray tube. In a further contribution, Nikitiana et al. 126 gave details of a new portable XRF analyser based on this configuration using a lens capable of achieving a 10 μ m focal spot. Gormley *et al.* ¹²⁷ studied the spectral gain function of polycapillary X-ray optics designed for use in conjunction with both Mo $K\alpha$ and Cu $K\alpha$ sources. They reported that although individual capillaries were tapered, their performance could be described by a simple parabolic relationship between the radius of curvature and the maximum energy transmitted for capillaries of constant diameter.

Single glass ('monolithic') capillary waveguides also continue to attract interest. Ding et al. ¹²⁸ discussed advances in the use of monolithic capillary X-ray lenses in XRMF and XRD applications. Arkadiev et al. ¹²⁹ described a table-top instrument with a spot size of about 100 µm incorporating a high brilliance, low power, X-ray source and integral optical microscope. Commercial instruments having a similar config-

uration are available for applications such as the analysis of single particles or high local resolution of larger samples, and one such instrument was described by Haschke and Theis.¹ Another, with a similar configuration, was described by Nicolosi et al. 131 and offered a spatial resolution of 5 μm. An experimental comparison was undertaken by Kanngiesser et al. 132 into the performance of a capillary 'lens' against a highly orientated pyrolytic graphite (HOPG) toroid designed for focusing Mo Kα radiation, and between a capillary and a multilayer optic designed for use with Mo Lα. The range of applications of these devices and useful configurations of instrumentation were discussed. Instrumentation incorporating monolithic capillary optics was also used in various applications, including the work of Wegrzynek et al., 133 who measured the distribution of elements including Br, Hg, Pb in polymer films using an instrument capable of achieving a 50 µm spatial resolution. This study was targetted at measuring the distribution of both additives and contaminants introduced during the polymer film manufacturing process.

4.3 X-ray microfluorescence

An interesting *instrumental development* was described by Ohara¹³⁴ in terms of a spectrometer designed for light element microanalysis. The instrumentation incorporated an X-ray collection/collimation optic designed to collect a large solid angle of sub-keV X-rays from a sample and convert it into a parallel beam and was designed for a range of X-ray and electron microprobe applications.

Of the range of *applications* available for review, Cheburkin and Shotyk¹³⁵ described the analysis of 100–150 µl water samples using a system comprising a 2 kW Mo anode X-ray tube, a focused LiF(220) curved crystal monochromator and a 28 mm² Si(Li) detector. Samples (e.g., glacial waters and digested peat samples) were evaporated onto PTFE film which served as the sample support membrane and results for up to 13 elements were reported in the range 20–700 pg ml⁻¹. One advantage of this technique in comparison with TXRF was claimed to be the fact that detection limits were less dependent on the concentration of the matrix, permitting the technique to be applied to samples ranging from rainwater to acid digests of biological and geological samples. Schmetzer et al. 136 used XRMF and EPMA to characterize zoning in trapiche rubies (these are rubies that have a clear central region, but zoned outer regions), producing 2-dimensional maps for Al, Ca, Cr, Fe, Si and Ti. Elemental imaging was also the theme of a paper by Havrilla and Schoonover, 137 who described the advantages of integrating elemental and molecular images produced by XRMF, micro-Raman and micro-IR to complement conventional spectroscopic analytical methods.

Hammersberg et al. 138 undertook a more fundamental study in measuring the absolute energy spectra for an industrial tungsten-anode microfocal (5 μ m) X-ray tube source as a function of tube potential (30–190 kV). This study was designed to contribute to an assessment of the dependence of image quality on X-ray instrument parameters in applications such as CT, although it also has wider relevance in XRMF.

In terms of *subject reviews*, 'X-ray Microanalysis in Biology' is the title of a book edited by Sigee *et al.*¹³⁹ that includes comprehensive coverage of a range of X-ray microanalytical techniques to facilitate research in the biological sciences. Chevallier *et al.*¹⁴⁰ also published an overview, but in this case of developments in X-ray optics and of XRF microprobe analysis systems which have resulted from the advent of SR sources, a review that represents a particularly good link to the next section.

5 Synchrotron radiation

World-wide, the number of synchrotron storage rings and beamlines available for XRF studies and applications is increasing to take advantage of the unique properties of the synchrotron as an X-ray source. These unique properties include the natural high degree of collimation, high degree of linear polarization, wide spectral range with energies from eV to 100s of keV now available and, most importantly, very high brilliance (up to 10^{18} – 10^{19} photons s⁻¹ mrad⁻² mm⁻² (0.01% band width)⁻¹, which is 9–10 orders of magnitude greater than that from an X-ray tube. Publications over the last year reflect the continuing importance of fundamental studies, but synchrotrons are increasingly being used for applied research and industrial applications. One of the more exciting developments is the use of SR beamlines as a source for TXRF studies. These aspects are covered in detail in the TXRF Section 6.

5.1 Beamlines and optics

Freund¹⁴¹ presented a review article about synchrotron X-ray beam optics with emphasis on the special requirements due to the low emittance and the high brilliance of third generation storage rings. Sutton and Rivers¹⁴² reviewed hard X-ray synchrotron microprobe techniques and applications in an area which is much more demanding than with soft X-rays because of the more demanding physical tolerances necessary to achieve the focusing effect. Adams¹⁴³ also reviewed aspects of SR as a tool for microscopic analysis, in particular considering the possibilities of the new third generation synchrotron storage rings, especially the European Synchrotron Radiation Facility (ESRF).

Turning now to more specific aspects of beamline optics, Sellschop described the production of synthetic diamond single crystals for use as high quality elements in beamline monochromators that were capable of resisting the intense Xray fluxes produced by modern SR sources. Freund et al. 145 continued this work by incorporating these devices in a synchrotron X-ray beamline, demonstrating the high quality of the 111-orientated diamond crystal (having an area of up to 50 mm² and thickness 67–175 μm) as a monochromator. An impressive outcome of this investigation was that the rocking curve width exceeded the theoretical value for a perfect crystal by only a couple of arc seconds. Lang et al. 146 investigated the improvements based on the bending magnet beamline 1-BM at the Advanced Photon Source (APS). They showed that a Si(111) focusing monochromator was capable of delivering a flux of $9 \times 10^{1\overline{1}}$ photons s⁻¹ $(100 \text{ mA})^{-1}$ at 10 keV with an energy resolution of $\Delta E/E = 1.5 \times 10^{-4}$, which is extremely high for a bending magnet beamline.

A computer code for the computation of synchrotron radiation and a graphical user interface for the calculation of spectral distributions, multilayer reflectivities, crystal diffraction profiles, *etc.*, were developed by Chubar and Elleaume. ¹⁴⁷ The particular feature of this code was that it was capable of computing SR spectra from relativistic electrons with high precision and efficiency in the near and far field range. Two examples were presented illustrating some unexpected properties of the focusing of radiation from a bending magnet and an undulator. Sanchez Del Rio and Dejus¹⁴⁸ also developed a computer program with a graphical user interface to run computer programs that calculate the basic information required to design SR beamlines. This software had the capability of calculating crystal diffraction profiles and multilayer reflectivities and, with some limitations, is available free of charge from the authors.

5.2 SRXRF instrumentation

Turning now to instrumentation designed for SR beamlines, Hayakawa et al. 149 described a wavelength dispersive X-ray

spectrometer developed for microanalysis on the undulator beamline at Spring-8 (beamline 39XU) and presented preliminary results on its performance. This instrumentation incorporated a flat Si(111) analyser crystal and a position sensitive proportional counter placed behind a movable 50 µm slit and was tested by measuring resonant inelastic X-ray scattering from a nickel foil. The development of a multipurpose XRF analyser designed for both XRF and TXRF of microsamples using either a conventional X-ray tube or SR source (see section 6.2) was described by Terada et al. 150 The instrument was used to analyse cosmic dust samples collected in Antarctica with a conventional X-ray source. To show the potential of this analyser in TXRF mode using a third generation SR source (Spring-8), standard river water samples were analysed and an evaluation of performance showed that exceptionally low detection limits of down to 10 fg could be achieved. Sakurai¹⁵¹ gave details of the development of a Johansson-type spectrometer for use with monochromatic radiation from an undulator source. The spectrometer, which incorporated a Ge(220) analyser crystal, was reported to achieve an energy of 8 eV for Cu $K\alpha_1$ line (8.04 keV). The XRF beamline at the Brazilian SR facility LNLS was described by Perez *et al.* 152 This facility used a Si(111) channel-cut monochromator as the main optical component to tune the beam energy to 3-14 keV for TXRF and XRF microprobe analysis. By combining micro-XANES and micro-SR-XRF using a SR source, it becomes possible to undertake the microprobe analysis of elements as well as to obtain information on the chemical state and local structure (including inter-atomic distances and coordination number), an important advantage of SR XRMF instrumentation. These possibilities were investigated by Mosbah et al. 153 in the analysis of the oxidation state of iron in glass inclusions trapped in volcanic minerals to provide information on the evolution of magmas.

5.3 Applications

Takada et al. 154 exploited the advantages of SR-XRF by presenting the results of the imaging of a single brain cell from patients with Parkinson's disease. The aim of the study was to provide data on whether the accumulation of trace metal elements (especially Fe) has a strong influence on the degenerative process associated with this disease. Results were presented for the elemental mapping of a $100 \times 100 \,\mu\text{m}^2$ area of a neuron, excited by a $6 \times 8 \mu m^2$ X-ray probe of 13.5 keV energy. Hansteen *et al.* 155 conducted a systematic study of the performance of a synchrotron XRF microprobe in the analysis of geological reference materials prepared as glasses and reported repeatabilities of better than 1% (RSD) for elements present at concentrations greater than several µg g and accuracies of typically 0.25-14%. A particular feature of this work was the capability of measuring trace element K lines in the range Cu-U and the authors concluded that SR-XRF was well suited to studies of trace element zoning and diffusion in geological samples. Fossilized bone samples were analysed in cross section by Janssens *et al.*, 156 who were particularly interested in recording profiles of the REEs at concentrations above 10 μg g⁻¹. Samples were analysed using conventional geometry with a white X-ray beam which was filtered using an 8 mm thick Al plate to suppress the low energy spectrum and adjusted to give a spatial resolution of 20-30 µm using an adjustable collimator.

Other applications included the work of Nozaki et al., 157 who determined trace element abundances in cosmic spherules collected from deep sea sediments. Results indicated that spherules could be divided into two groups, one with high and the other with low Mn content. They hypothesised that the low Mn group were associated with iron meteorites that had lost volatile elements during melting but that the high Mn group could not be identified with any formation process. Figueiredo

et al. 158 undertook elemental mapping of selected geological minerals by SRXRF to provide information on the influence of size and orientation of single mineral grains. The morphological distribution of inorganic elements in wood was investigated using microbeam SRXRF by Berglund et al., 159 taking advantage of the non-destructive capabilities of the technique to permit analysis of the sample before and after chemical treatment. Some differences in the distribution and concentration of certain metals was observed when samples were subjected to treatment with an EDTA solution. SIMS and SRXRF were used to measure the metal content of ring systems in trees from Northern Canada by Martin et al. 160 The aim of this study was to show seasonal variations in the uptake of metals.

6 Total reflection X-ray fluorescence

During the current review period the proceedings of the 7th Conference on TXRF and Related Techniques, which took place in Austin, Texas, were published as a special issue of Spectrochimica Acta, Part B. 161 The papers in this issue sum up the variety of new developments and applications as well as technical improvements, many designed for Silicon-wafer surface analysis for the semiconductor industry. Some contributions mentioned in last year's ASU review as conference contributions were published therein.

6.1 Instrumentation and quantification

A total-reflection *imaging system* was developed by Sakurai, ¹⁶² consisting of a rotating copper anode source, a Si(111) channel-cut monochromator, a capillary collimator for the fluorescence photons and a CCD camera, and offered spatial resolution of 40–50 µm. Using tunable monochromatic SR, the system could be used to record images of specific elements by selective excitation.

Several developments dealt with techniques for increasing the primary intensity in TXRF instrumentation. The TXRF group at GKSS published a paper¹⁶³ describing a tunable focusing monochromator for use with W-L β and Mo-K α excitation. After optimization of all parameters of the monochromator, the authors reported an improvement of 43% for 9.67 keV W-Lβ and an improvement of 27% for 17.5 keV Mo-Kα excitation, as compared with results obtained using flat mirrors. The group at the Atominstitut in Vienna¹⁶⁴ described a simple method to increase sensitivity by mechanically bending a multilayer monochromator to the shape of a logarithmic spiral. This led to a larger angle of acceptance that met the Bragg condition and gave an intensity gain by a factor of 3 for 17.5 keV radiation. Tsuji, together with colleagues of the Antwerp group, 165 reported experiments using two X-ray beams for excitation of the same sample. A rotating anode tube with a molybdenum target and a glow discharge tube with an iron target were used to excite Cr fluorescence radiation from a thin film sample on a quartz carrier. It should have come as no surprise to the authors that an enhanced fluorescence signal was observed in comparison with excitation using only one tube.

Another active topic of research was the *comparison in performance of spectral modification elements and sample reflectors*. Excitation with monochromatic excitation was compared with that using a cut-off mirror by Padilla Alvarez *et al.*, ¹⁶⁶ who drew the conclusion that for low Z elements, the cut-off mirror led to better detection limits, but for elements from Fe to Y, monochromatic excitation using a rubidium acid phthalate (RAP) crystal provided best results. A double reflection module was used by Filho *et al.*, ¹⁶⁷ consisting of two 100 mm long quartz crystals placed 50 µm apart. An impressive detection limit of 4 ng ml⁻¹ for Zn using a sample volume of 50 µl was obtained. Theisen *et al.* ¹⁶⁸ tested sapphire

as a sample carrier for TXRF and reported that it was similar to standard reflector materials, but with the advantage of allowing the determination of Si. By varying the angle of incidence for each type of sample carrier, Prange *et al.*¹⁶⁹ were able to improve the peak-to-background ratio. The use of such optimization is already widely used by those assembling their in-house TXRF equipment. In a related contribution, Knoth *et al.*¹⁷⁰ calculated the background as a function of the incident angle for various sample carrier materials.

An interesting approach to *quantification* was published by Szaloki *et al.*¹⁷¹ based on fundamental parameters, as well as geometrical parameters. The latter were determined using the Si K line signal from the sample holder. The authors claimed not to need external or internal standards for calibration.

The group of the Atominstitut, Vienna, ¹⁷² published results of their investigations of *low Z elements* (Al, C, Mg, Na) and reported improvements in excitation conditions using SR and applications to wafer surface analysis, as well as depth profiling. In addition, the first successful application of a standard fine-focus chromium anode tube to the analysis of aerosols was reported.

6.2 Synchrotron radiation induced TXRF

The installation of a new grazing incidence X-ray spectrometer and reflectometer on beam line 39XU of Spring-8, at the moment the most advanced storage ring in the world, was reported by Sakurai et al. 173 The instrument is planned to be used for surface/interface morphological studies by specular and non-specular X-ray scattering, but currently only preliminary results have been reported.

Progress in the *analysis of wafer surfaces* was reported by two groups. Comin *et al.*^{174–176} reported on the planned impressive and highly elaborate industrial SR-TXRF facility at ESRF, Grenoble. Mapping of surface impurities (Na to Hg) on 300 mm silicon wafers is expected to provide detection limits <10⁹ atoms cm⁻². Under optimized conditions, detection limits of <10⁸ atoms cm⁻² were expected. The wafer was to be mounted horizontally and two 7 Si(Li) detector arrays would be mounted along the polarization direction. The authors claimed that the facility would analyse three wafers per hour. A special fixed-exit monochromator was developed, covering the energy range from 1–40 keV and incorporating a Si(111) channel-cut monochromator as well as a multilayer pair. Kim and Ryoo¹⁷⁷ from the Korean Institute of Industrial Science and Technology also published results on SR-TXRF applied to wafer surface analysis.

An improvement in instrumentation to facilitate faster set-up and alignment was reported by the Atominstitut group in Vienna, ¹⁷⁸ who used a fixed exit double multilayer monochromator, which was tested successfully at HASYLAB, Hamburg. Shin *et al.* ¹⁷⁹ investigated the background in SRTXRF spectra induced by photoelectron bremsstrahlung. They compared their theoretical results with experimental data and discussed conditions to reduce detection limits, which was investigated years ago by Takaura at SSRL.

Working at SSRL, Stanford, CA, Kregsamer *et al.*¹⁸⁰ reported the application of SR-TXRF to depth profiling and thin film analysis of *light elements*. This was the first time light element depth profiling had successfully been achieved.

6.3 Surface analysis

Huber and Freudenberg¹⁸¹ presented a fully automated wafer surface analyser, based on the vapour phase decomposition (VPD) preparation technique. Even the essential, but very challenging, *low Z contaminants Na and Al* could be included in the analysis. This extension to the light elements was achieved by using two TXRF chambers, one dedicated to the light elements and other to the normal range of elements. When the

VPD method was used in combination with TXRF analysis, accurate positioning of the sample droplet was found to be important. As a result of this development, a special search routine was developed by Funahashi *et al.*¹⁸² to optimize sample positioning. In a Japanese language article, Yamagami *et al.*¹⁸³ claimed detection limits for Na and Al as low as 3×10^{10} and 2×10^{9} atoms cm⁻², respectively, for 150 mm silicon wafers. Several other authors used VPD TXRF for trace element analysis on silicon wafers^{184–186} and silicon nitride films.¹⁸⁷

Depth profiles of co-implanted silicon wafers were reported in publications by Klockenkämper et al., ^{188,189} who applied TXRF after repeated stratified etching. The TXRF results were compared with the results from Rutherford backscattering and were found to agree quite well. Rink and Thewissen¹⁹⁰ applied variable incidence angle TXRF to establishing whether As contamination was in or on the silicon wafer surface. Iltgen et al. ¹⁹¹ presented examples of angle-resolved TXRF for the determination of the implanted dose and surface roughness for monitoring ion implantation, thermal annealing and polishing processes. TXRF and TOF-SIMS were compared by Iltgen et al. ¹⁹²

Mori et al. 193 reviewed error factors in quantitative TXRF, including source stability, accuracy of mechanical positioning, spurious peaks and surface roughness. In this context, Liou and Lee 194 proposed a method designed to reduce spurious peaks by orienting the wafer so that the (100) crystal plane was aligned in a chosen direction with respect to the incident beam, a development that has already been suggested by Japanese groups. Werho et al. 195 used heavy ion backscattering spectrometry to standardize TXRF calibration samples, which ensured that all TXRF instruments within a wafer company provided consistent analytical results. The same group questioned if TXRF instruments could be used reliably as true in-line analytical tools, due to contamination problems. 196

6.4 Related techniques

Grazing emission XRF (GEXRF) with 90 degrees incidence and a shallow angle of detection is an alternative to TXRF for the surface characterization of certain samples. In this geometry, detection of the fluorescence signal is possible with WD methods, which is claimed to be particularly favourable for the determination of the light elements. The Antwerp group 197 investigated the influence of organic matrices on the determination of trace levels of Na, Pb and Zn and found detection limits of 0.4, 2 and 1.5 ng, respectively. Applications reported by members of this group included artists' pigments, 198 light elements in marine aerosols, 199 beer samples 197 and Si in organic matrices, e.g., liver, cellulose, urine, serum, spinach, beer and mineral water. 200 A review article was presented by Claes et al. 201 which emphasised developments in and applications of GEXRF.

Ultra-thin nickel thin films sandwiched with carbon thin films of different thickness were measured by Tsuji et al. 202 The Ni K α intensity of the Ni ultra-thin film sandwiched with carbon layers was 3 times enhanced in comparison with the Ni fluorescence from the Ni film without carbon layers. The enhancement was caused by standing wave interference effects on the surface of the substrate. Such a structure offers interesting possibilities for use in monochromators to deliver increased output intensity.

Simulation was used by Spolnik and co-workers²⁰³ to study *quantification in GEXRF*. Calibration plots were linear for layers less than 1 nm thick. For thicker layers, deviations were predicted to arise due to absorption and variations in standing wave fields. It was proposed by Kuczumow *et al.*²⁰⁴ that several problems in quantification should be tackled by empirical rather than theoretical approaches, namely the calibration and

the standard addition method. For the determination of depth profiles by GEXRF, the inverse Laplace transformation can be used. It is well known that the problem is ill-posed and hence the solution is not unique. Therefore, two methods to determine the regularization parameter were studied by Kok and Urbach.²⁰⁵ These authors concluded that it should be possible to reconstruct the profiles providing the X-ray source was sufficiently intense to produce strong fluorescence signals.

Grazing exit electron probe microanalysis (GE-EPMA) was reported by Tsuji et al. 206 For this technique, electrons are used to excite the sample and, due to the shallow angle of detection, the resulting background is much lower than in standard EPMA. The characteristic radiation was detected using an ED detector 207 and the system was used to analyse aerosols on silicon wafers. This is the first report of elemental X-ray imaging using this new technique.

6.5 TXRF Applications

In the field of *sample preparation*, a new electrochemical enrichment procedure for the determination of heavy metals by TXRF was developed by Ritschel *et al.*²⁰⁸ from the Atominstitut group, Vienna. Mercury was electro-deposited from a sample solution containing Te as an internal standard on to a niobium disc electrode and then determined. The calibration graph was linear up to 500 ng l⁻¹ of Hg and an impressive detection limit of 4 ng l⁻¹ was achieved. Bennun *et al.*²⁰⁹ described a method to determine Hg using amalgamation with Au. An amalgam was formed on a thin gold layer on a quartz reflector while in contact with a Hg ionic solution. To obtain better precision, a special data processing method was applied to solve the problem of peak overlap between Hg and Au L lines.

A comparison of sample preparation methods for *aerosol analysis* by TXRF was performed by Theisen *et al.* 210 in which oxygen plasma ashing on sapphire carriers was compared with the acid digestion of airborne dust samples on cellulose acetate filters. Dixken and Fissan 211 developed an electrostatic precipitator as sample collector for off-line particle analysis. These authors optimised the collection efficiency and the deposition pattern and tested the instrument for particles from 0.03 μm to 10 μm . Vilhunen and co-workers at ISAS, Dortmund, 212 determined Ca, Cr, Cu, Fe, Mn, Ni, Pb, S and Zn in exhaust particles from two diesel fuels of different S content. A reduction of total particulate emission was found when a fuel with very low S content was used.

Turning now to *beverages*, bromate ions in drinking water were determined by Kallithrakas-Kontos and Kavelaki. ²¹³ A combination of an ion chromatography separation with TXRF was used and ng g⁻¹ levels were determined. Bakraji and Karajo²¹⁴ determined heavy metals in Damascus drinking water with detection limits of 0.1–0.4 μ g l⁻¹. Using a similar simple, low cost, TXRF attachment module, Capote *et al.* ²¹⁵ determined Cu, Fe and Zn in spiritous beverages with detection limits of 22, 20 and 19 μ g l⁻¹.

TXRF was applied to *environmental investigations* by members of the Chalmers University group, ^{216,217} who analysed Scots pine needles and fine roots of Scots pines. The authors reported good agreement with results from ETAAS. Holynska *et al.*²¹⁸ used a chemical separation method to perform speciation of heavy metals in peat with TXRF.

Estuarine sediments and water samples were analysed by members of the Lisbon group after sample preparation. The data were used to determine the extent of industrial pollution associated with the Tagus River near Lisbon. Using TXRF, high concentrations of As and Pb were detected in sediments with As and Fe found to be above recommended values in water.

A novel application of TXRF was the trace metal uptake and

transport processes in cucumber plants, which was studied by Varga et al.²²¹ The authors specifically assessed the contamination effects of Cd, Ni, Pb and V. Tatar et al.²²² investigated the effect of contamination of Ni, Pb and V on organic acid transport in xylem sap of cucumber.

In the field of medical and biological applications, TXRF was used for the analysis of human blood serum and human brain samples. Marco *et al.*²²³ determined Cu, Fe, Pt, Se and Zn in serum and Cu and Zn in brain tissue. The trace element load in cancerous and normal lung tissue was investigated by Kubala-Kukus et al. 224 using both TXRF and PIXE. The authors found that levels of Cr, Mn and Ti were enhanced by up to 48% in cancerous lung tissue taken from women. Conversely, levels of Pb and Sr were found to be up to 30% lower in women than men. Quantification of Pt bound to DNA was reported by Ruiz et al. 225 and TXRF was recommended by the authors to be a suitable technique for studying trace metals in a biochemical process. Bellisola et al. 226 studied the metabolism and excretion of Se in humans. The statistical distribution of trace element concentrations in biomedical samples was investigated by Majewska *et al.*,²²⁷ and TXRF results were compared with PIXE. Kelko-Levia *et al.*²²⁸ investigated the use of flow injection ion-exchange preconcentration techniques for the TXRF determination of trace elements in pharmaceutical substances and compared TXRF with GF-AAS. With this interesting combination, TXRF could be used for the important speciation studies of Cr^{III} and Cr^{IV} in these materials.

In the field of *cultural heritage*, Klockenkämper *et al.*²²⁹ demonstrated the extraordinary benefit of high sensitivity and multielement coverage provided by TXRF. Using only light contact with a cotton wool bud, sufficient material, *i.e.*, a few micrograms, was obtained for TXRF analysis and this procedure was readily accepted by museum curators. This technique was applied to the analysis of pigments on oil paintings and inks in historical manuscripts. Using a similar sampling approach that produced flakes of less than 20 µg, historical violin varnishes were analyzed by von Bohlen.²³⁰

7 Portable and mobile XRF

Portable XRF (PXRF) continues to be an exciting area of development where advances in technology can have a significant impact on instrument performance and practicability. One innovative development has already been mentioned in Section 2.2 concerning the work of Cesareo et al. 61 on the use of thermoelectrically cooled semiconductor detectors, such as CdZnTe and HgI₂, coupled to miniaturized X-ray tubes. In this work, the use of a Ca-anode tube to optimise the excitation of S caused by pollution in an old Roman fresco is particularly noteworthy. The instrumentation described by Fiorini et al.²³¹ incorporated a Si drift detector and results were reported on a range of different samples analysed in the field, including metal alloys. The PXRF analyser used by Khusainov et al.232 incorporated a CdTe PIN detector and was used for applications such as metal alloy verification at customs control, contamination (Hg, Pb, Th) in housing environmental control and Pb in gasoline, mining and nuclear material process control. Instrumentation based on the same CdTe detector type was developed as a gamma spectrometer. Although the use of gas proportional counters in PXRF applications is diminishing, Boyle⁸⁸ described an interesting development, which has already been referenced in Section 2.2, in signal deconvolution from such devices that was claimed to greatly improve the practical application of this PXRF instrumentation in the analysis of geochemical and environmental samples.

PXRF is one of a range of developing portable techniques that can be used for field measurements, so it is timely to read the work of Goldthorp *et al.*,²³³ who evaluated the range of 'person-portable' instrumentation available and their capabil-

ities. Instrumentation considered included portable gas chromatographs, Fourier-transform IR spectrometers and PXRF, each of which is capable of quantifying different groups of elements or species.

Mobile laboratories are, of course, the other way of making field measurements and Flachowsky et al.²³⁴ described such an on-site laboratory designed for the rapid turn round of samples in the characterization of waste sites using GC–MS as well as EDXRF instrumentation. Moreplavtsev and Tarakanovskii²³⁵ described a Russian instrument capable of determining Au down to the 0.01–3 g m⁻³ level in sandy ores for geochemical prospecting applications in a mobile laboratory.

Turning back again to in situ PXRF measurements, contaminated land is one of the most popular applications of the PXRF technique and Ridings et al. 236 considered appropriate strategies when using the technique to map the distribution of As at a disused plunge dip. In situ and ex situ measurements were compared and the option of using PXRF as an enhancement, rather than a replacement, for existing methods was demonstrated. Arsenic contamination is likely to become a growing application of PXRF and Schneider *et al.*²³⁷ used PXRF to measure such contamination resulting from the destruction of WWII chemical agents at a military site in Germany. Notwithstanding these developments, lead in contaminated soil continues to be the most common PXRF application. VanCott *et al.*²³⁸ investigated errors in determinations by PXRF in comparison with laboratory AAS using standard samples. Further comparisons with laboratory-based techniques were undertaken by Anderson et al. 239 in the analysis of industrial soils for a suite of elements (Cd, Cr, Cu, Mn, Ni, V, Zn). PXRF data were found to agree with certified values in soil reference materials within a factor of 2, a disappointing agreement. Further work with the cone penetrometer, designed to characterize sub-surface contamination, was published by McDonald *et al.*, ²⁴⁰ who presented results from bench testing and calibration using lead-contaminated calibration samples.

Many PXRF applications are related to studies that involve a risk assessment to identify whether contamination represents a significant *hazard to health*, and Clark *et al.*, from the University of Cincinnati, ^{241,242} reviewed the use of field PXRF measurements in lead-contaminated airborne dust filters, soils and dust wipes. In a further contribution from the same group, Morley et al. 243 used PXRF to determine Pb in workplace air samples, in this case air particulate filter samples collected at bridge blasting sites. On-site measurements by PXRF were followed up by laboratory graphite furnace AAS analyses as the reference method. No statistical difference was found between the two sets of measurements and the accuracy of the PXRF data was reported to be about $\pm 16\%$, with a detection limit of 6.2 µg of Pb per sample. These results indicated that an industrial hygienist could use the PXRF technique for rapid site assessments with the samples sent to the laboratory for subsequent confirmatory analysis.

An interesting comparison of field testing technologies for the determination of *lead in paint* was undertaken by Schmehl *et al.*,²⁴⁴ who compared the performance of six chemical test kits and six XRF instruments. The authors concluded that under real-world conditions, the chemical test kits were not effective in distinguishing lead-based paint in accordance with US Federal standards, but that in some circumstances the XRF instruments were effective.

The analysis of archaeological and museum samples and objects of art continues to be a fruitful area of application for PXRF and Cesareo (University of Sassari)²⁴⁵ described an instrument designed for the measurement of Cl, P and S to detection limits in the 0.03–0.04% m/m range. The instrument incorporated a Pd anode X-ray tube and a Si–PIN detector and was tested by analysing Cl and S contamination on frescoes and monuments. Vittiglio *et al.*,²⁴⁶ from the equally productive

University of Antwerp group, described a compact small-beam instrument using a mini-focus side-window Mo-anode X-ray tube and a Si-PIN detector. One interesting innovation was that two laser beams were aligned so that the point of intersection coincided with the tube-sample-detector axis, thus facilitating optimum alignment of the sample. The instrument was tested by analysing a series of standard brasses and a bronze and was then used for the analysis of archaeological bronzes from the Egyptian and Roman eras. Moioli and Seccaroni²⁴⁷ reviewed their work in the use of PXRF for the analysis of objects of art, including paintings, mosaics, glasses, ceramics, and bronzes. In some cases, PXRF data could establish the provenance of the materials or characterize differences in the same work due to restoration or the presence of unoriginal materials.

Perhaps one of the ultimate challenges of PXRF is in space research. X-ray spectrometers have for a long time been used for cosmic X-ray spectroscopy, instrumentation for which was reviewed by Fraser²⁴⁸ and Paerels.²⁴⁹ However, the 1997 Pathfinder mission to Mars provided some unique data on the composition of Martian soil obtained by an alpha-proton XRF spectrometer and a detailed geochemical interpretation of these data has been presented by McSween *et al.*²⁵⁰ and Newsome *et al.*²⁵¹ In anticipation of future space lander missions, Radchenko et al. 252 designed and manufactured open alpha sources, based on²⁴⁴Cm (185 MBq, 5 mCi), intended for the analysis of the elemental composition of the Mars surface rocks and atmosphere by alpha-backscattering, alpha-proton scattering and XRF. Conventional XRF analysis involves sending PXRF instrumentation to a planet's surface. However, an alternative approach is to use an X-ray spectrometer flown on a space mission in near orbit around the moon, a near-Earth asteroid or a comet to measure the XRF spectrum excited by the X-ray flux emitted by the Sun. The result would be a compositional map of the surface, providing valuable information concerning its evolution. A novel instrument suitable for such measurements was described by Martin et al.,77 based on microchannel plate optics and a CCD. A mission to map the elemental composition of the Moon's surface was described by Okada et al. 253 with the aim of estimating the average composition, distribution of rock types and the composition of lava flows and craters. This experiment is planned to be flown on the 2003 SELENE orbiter. And finally, Kamata et al. 254 presented results from the ASCA observation of the lunar surface during July 1993, based on the detection of Al and Si K X-ray fluorescence emissions which were very weak in comparison to the cosmic X-ray background level.

8 On-line XRF

Each year we remark on the small number of published contributions in the area of on-line XRF analysis, and although the same comments apply this year, again this should not be taken as an indication of the lack of importance of XRF in this area of application. One of the more interesting contributions was a patent application by Nelson²⁵⁵ for a compact XRF spectrometer for *real-time wear metal analysis of lubricating oils*. The sample chamber of this instrument was designed to be connected to the lubrication system of the machine to be monitored. The excitation source was designed to be either an X-ray tube (with a collimator or focusing assembly) or an X-ray laser source and the instrument incorporated a low-noise X-ray detector with an associated computer system for detecting the presence of and quantifying the amount of wear metal particles in the lubricant.

Use of the techniques of XRF and X-ray transmission (XRT) were reviewed by Tisdale²⁵⁶ for application in on-line process control in the *petroleum refining and petrochemical industries*, where many hundreds of working installations were

claimed world-wide, typically measuring $\mu g \, g^{-1}$ levels of contaminants. Interestingly, XRT was claimed to be best suited to the direct analysis of high temperature/pressure liquid streams, whereas XRF required sample conditioning and recovery systems for proper operation, since it is not yet possible to design an XRF flow cell window that is both sufficiently strong and reliable to withstand processing conditions and retain transparency to X-rays.

conditions and retain transparency to X-rays.

Turning now to *other applications*, Tisdale, ²⁵⁷ in a second contribution, reviewed advances in on-line XRF analysis for process control, covering the development of robust, highprecision EDXRF spectrometers, spectrum deconvolution and matrix correction software, the design and refinement of automatic sampling systems and feedback to the plant control system. Bachmann and Sauer²⁵⁸ described an online XRF system for the measurement of S in coal (and Ca, Fe and Ti in coal ash) and Pedersen and Finney²⁵⁹ described, in a Spanish contribution, the performance of a commercial on-stream XRF analyser incorporating a windowless powder flow cell in one of the traditional areas of application, the cement industry. Nahle et al.260 considered X-ray design constraints for in situ electrochemical cells, specifically the need to measure X-ray absorption losses in a range of polymer window materials used in such applications. On-line monitoring of flue gas emissions by EDXRF was reported by Harmel et al. 261. The sampling and analysis system was found to monitor successfully a range of elements from atomic number 19 (K) to 82 (Pb) in ambient air. In another paper²⁶² by this group, calibration of the spectrometer was described.

9 Applications

9.1 Sample preparation

It is pleasing to report that a technique introduced in last year's review on the analysis of liquids by drying microdroplets has been further developed during this review period; Colletti and Havrilla²⁶³ investigated parameters affecting the qualitative capabilities of the dried spot method. These parameters included choice of thin film substrates, drying methods, solution composition and solution containment. Sugihara et al. 264 focused their work on the polyamide support film and its effect on the background from scattered radiation. Wilson et al.265 evaluated a new support film (AP2) with temperature tolerance and chemical resistance, designed to minimise the contribution to background scatter. Their work reported repeatability data that demonstrated the residue-locating properties of dimpled and treated films. Yamaguchi et al.²⁶⁰ preferred filter papers and specified different types for a range of applications.

The demands for reproducibility and consistency of analytical results for the *analysis of cement* were addressed by Wachal and Reister. ²⁶⁷ An upgrade of their automated sampling and sample preparation line resulted in a change from pressed pellets to fused beads with a strong improvement in quality control performance.

Kurunczi et al. ²⁶⁸ described a method for the determination of *Hg in waste flue gases* using galactose impregnated filters treated with Brashear's silvering solution. The reader is advised on ageing effects of the filters, which is often a concern for workers using this method of sample preparation.

9.2 Preconcentration techniques

In an extension of earlier work, McComb and Gesser²⁶⁹ investigated the feasibility of using a poly(acrylamidoxime) cloth for *in-situ* sample preconcentration of *trace analytes in water*. Uptake of Cd, Cu, Fe, Mg, Mn, Pb and Zn was assessed by *in vitro* experiments in which solutions of these elements were passed through a flow chamber containing samples of the

chelating cloth, which were subsequently analysed by both XRF and ICP-AES, the latter after extraction of the metals from the cloth using 1% v/v nitric acid. Good agreement was reported between the passive monitors and field tests for trace metals in river water. De Vito et al. 270 used a new chelating resin loaded with thorin for the determination of the trace rare earth elements, Eu, Gd and Sm, from aqueous solutions. The method was applied to the geological reference material USGS G2 showing good agreement with certified values. Makar-ovskaya *et al.* ²⁷¹ described a method of manufacturing thin film samples from organic extracts based on a block copolymer of polysiloxane and polycarbonate. The procedure was used for the solvent extraction of As and Se in drinking water. In another contribution from the National Academy of Science of Ukraine, Belikov and colleagues²⁷² described the determination of mobile forms of Co, Cu and Zn in soils using preconcentration on silica gel modified by didecylaminoethyl--tridecylammonium iodide. The influence of foreign ions on the completeness of the sorption was also studied.

9.3 Geological

As was hinted in last year's review, the use of XRF techniques in the geological field is now well established, with very little innovation possible. This was again in evidence this year with a remarkably low contribution to this area. As can often be expected the predominant feature was the analysis of rocks and minerals. El Maghraoui et al.²⁷³ reported the use of WDXRF and INAA in a 'round robin' exercise to establish the concentration of 44 major and trace elements in a series of magmatic rock reference materials. XRF analysis was carried out on samples prepared either by fusion [1.5 g with 9 g flux 120A (90% lithium tetraborate and 10% lithium fluoride)] or by pressed disc (4 g sample + 0.4 g wax). The ability of WDXRF to provide precise quantitative data for the determination of Nb in rocks at very low concentration was demonstrated by Etoubleau *et al.*²⁷⁴ A standard addition procedure with careful selection of peak and background line and a separation procedure based on that by Rehkamper (1994), followed by collection of Nb on an anion-exchange membrane, were both evaluated and results from both techniques compared. Figures obtained from the ion-exchange method were reported to be approximately 10-15% lower than those by standard addition and data for 15 international reference materials were shown to be in good agreement with literature values. Indium and gallium were the trace elements of interest to Masi and Olsina.²⁷⁵ Their method applied to geological samples and USGS rock reference materials utilized a pre-concentration technique with chelating macroporous resins loaded with 5phenylazoquinolin-8-ol. Detection limits of 98 and 81 ng ml⁻¹ were reported for Ga and In, respectively. Although not appearing to show anything Earth-shatteringly new in terms of methodology, the article by Wheeler²⁷⁶ on the analysis of limestones and dolomites is of interest for its examination of sources and uses of calcium in cement and lime plants. Perhaps the most innovative application in this section was the use of a single low dilution lithium tetraborate fusion technique presented by Johnson and colleagues²⁷⁷ at the GeoAnalytical Laboratory, Washington State University. Utilizing a 2:1 flux to sample ratio, the authors reported results for the analysis of 27 major and trace elements in rock and mineral reference materials with no loss in precision or accuracy when analysed results were compared with both accepted values and results from other techniques in other laboratories. Borkhodoev²⁷⁸ undertook a systematic examination of problems in the X-ray fluorescence analysis of rocks.

Two papers described the use of XRF in the analysis of *soils*, *silts and sediments*. The first, by Aisueva and Gunicheva, ²⁷⁹ showed the development of a non-destructive procedure for the determination of major and trace elements in soils, sediments

and loose deposits. Other than drying at 105 °C, no sample pretreatment was required. The report also discussed the reasons for not using fusion techniques and how α -correction matrix corrections are applied. In the second paper Szaloki *et al.*²⁸⁰ utilized EDXRF and ICP-AES to investigate the geochemical composition of lake sediments from a peat bog in north-eastern Hungary. ICP-AES was used to analyse the soluble components and EDXRF the insoluble residue.

The application of an EDXRF emission-transmission technique utilizing an annular ¹⁰⁹Cd excitation source for the analysis of *geological and biological reference materials* was reported by Funtua. ²⁸¹ Soil (SOIL-7), lake sediment (SL-1), animal blood (A-13) and hay (V-10) from the International Atomic Energy Agency were analysed after pelletizing (0.3 g with 3 drops of an organic solvent). A thick foil of pure Mo was placed behind the sample as a target material for absorption correction and calibration was carried out using high purity metal foils or stable chemical compounds. All elements showed good agreement with certified values except those in the low energy region, where significant variation was noted.

Finally, the influential *Analytical Chemistry review* on geochemical and cosmochemical materials was published by Lipschutz *et al.*²⁸² This review not only considered XRF, but also the full suite of techniques relevant to the analysis of this category of sample.

9.4 Environmental

The application of XRF to the analysis of aerosols and air particle pollution continues to be reported in the literature. Readers wishing to appraise themselves of the principles and practice may benefit from a comprehensive review paper by Watson *et al.*²⁸³ Matsuda *et al.*²⁸⁴ used both XRF and ion chromatography to analyse Al, Cl⁻, K, Mg²⁺, Na⁺, NH₄⁺, NO₃⁻, Si, SO₄²⁻ and Zn in atmospheric aerosols collected on the roof of a 59 m high building in the centre of Tokyo. During a 12 month period, the authors were able to relate analysed components to seasonal changes. Fang et al. 285 used a multitechnique study for the inorganic and organic analyses of aerosols collected on the east and west sides of Hong Kong during a dust episode. X-ray fluorescence results showed pronounced increases in the relative abundance of Al, Ca, Cl, Fe and S when compared to non-episodic samples. Complementary data were obtained by ICP-MS and the origin of the dust was traced to Northern China. Steinhoff et al. 286 used Digitel high volume samplers to collect ambient aerosols on quartz fibre filters. Standard filters prepared from NIST SRM 1648 urban particulate were used by Wang et al. 287 to calibrate both XRF and LA-ICP-MS spectrometers for the determination of Si in airborne particulate matter collected from a heavily polluted metropolitan area of Kaoshiung, Taiwan. The same reference material was used by Talebi²⁸⁸ to determine the Pb content of airborne particulate matter. A comparison of WDXRF and FAAS showed good agreement. The author recognized the merits of XRF, with no time consuming sample preparation or use of environmentally unfriendly solvents. Sixteen elements, Br, Ca, Cl, Cr, Cu, Fe, K, Mn, Ni, Pb, Rb, S, Sr, Ti, V and Zn, were quantified by Bandhu *et al.*²⁸⁹ using EDXRF and PIXE techniques. The aerosol samples were collected from industrial, commercial and relatively cleaner zones in the city of Chandigarh, India. Soil dust was found to account for the major fraction of the measured mass, with industrial activity, vehicular traffic and refuse burning also identified as plausible sources. The chemistry and microscopy of atmospheric particles were studied by Chabas and Lefevre² in order to explain the weathering mechanisms of marbles and granites at the Delos archaeological site (Cyclades, Greece). Seneviratne et al.²⁹¹ published their study of air particulate pollution at an urban residential site in Colombo, Sri Lanka. Analysis by EDXRF indicated that the probable origin was

soils distributed as a result of wind and traffic. Cadle *et al.*²⁹² published a study to characterize particulate matter emissions from 195 gasoline and diesel passenger vehicles in use during the summer of 1996 and the winter of 1997 in Denver, Colorado. Zamurs *et al.*²⁹³ studied real-time measurement of Pb in ambient air during bridge paint removal. Once again, the reliability and practical application of the XRF technique was shown to be effective.

The XRF technique was also widely used for the assessment of marine pollution. Mendoza et al. ²⁹⁴ studied marine pollution indicators using EDXRF to assess microalgae, marine algae, marine sediments and corals. Several methods were investigated, including external standardization, fundamental parameters with Fe as the reference element and an absolute measurement based on spectrometer sensitivity. Orlic and Tang²⁹⁵ published their work on elemental depth profiles in marine sediments of Singapore coastal waters in which the combined strengths of PIXE, Rutherford backscattering (RBS) and XRF were used to determine elemental concentrations of >30 elements with detection limits as low as a few μg g⁻¹. Pollution assessment in the Trancao river basin in Portugal was investigated by Pinheiro et al., ²⁹⁶ again using PIXE, EDXRF and isotopic analysis (¹⁸O: ¹⁶O ratio).

Other studies involving the *analysis of aqueous samples* included Wehausen *et al.*, ²⁹⁷ who presented a method for the determination of major and some minor ions (Br⁻, Ca²⁺, Cl⁻, K⁺, Mg²⁺, Na⁺, SO₄²⁻, and Sr²⁺) in marine pore waters. The precision and accuracy of XRF were found to be comparable to those of common titrimetric, colorimetric, spectrometric and ion chromatographic methods, which are generally used for such matrices. Ellis *et al.* ²⁹⁸ described a method using EDXRF to meet the challenge of analysing toxic elements in hazardous liquid waste. Schoonover and Havrilla²⁹⁹ used both XRF and vibrational microscopy to assess highly heterogeneous actinide contaminated precipitates separated from brine storage solutions.

The multi-disciplinary approach again featured in a publication by Janssen *et al.*, ³⁰⁰ who used XRF and AAS to determine heavy metals in *sewage sludge*. Also, Beckers *et al.* ³⁰¹ used both XRF and GC-MS to investigate the pyrolysis of dried sewage sludge as well as lacquered wood and linoleum. Vapour from the pyrolysis process was upgraded using a regenerating cracking catalyst and the purpose of the study was to gather information about the effectiveness of the pyrolysis of waste material of biogenic origin.

Four papers devoted to the analysis of coal and fly ash were offered to the reader during this review period. Kierzek et al. 302 used the combined powers of gamma-ray spectrometry and both EDXRF and WDXRF to study sulfur, light and heavy metal analytes and naturally occurring radioactive isotope contents of coal and ash from eight different mines in the Upper Silesian Coal Basin, Poland. The results assisted in the selection of the most suitable coal for burning in electric power and heat plants to minimise environmental pollution. Sprta et al. 303 determined total sulfur in fly ashes from North Bohemian brown coals. Coal ash was the medium of interest to Zhang et al.,304 who devised a method for the determination of Ge in coal ash using WDXRF. Synthetic coal ash reference samples were prepared by fusing one part of sample to nine parts flux (Li₂B₄O₇/LiBO₂) and matrix corrections were applied using the Compton peak method. As a result, the calibration line had a correlation of 0.999 and was applicable to Ge contents in the range from 10 to $12\,000\,\mu\mathrm{g}\,\mathrm{g}^{-1}$. Karayigit *et al.*³⁰⁵ assessed Eocene coals from the Sorgun Basin in Turkey for environmentally sensitive trace elements using an energy dispersive polarized spectrometer, results being reported on a whole coal dry basis.

Mobile forms of Co, Cu and Zn in *soils* were investigated by Belikov *et al.*²⁷² Both soils and plants were examined for the effect of Pb pollution at various locations near the highway of

Ankarat, Istanbul, by Tekin and Tan.³⁰⁶ Kalinin *et al.*³⁰⁷ reported an environmental survey of heavy metals in rock, soil and water samples. Anderson *et al.*²³⁹ used AAS, ICP-AES and XRF to determine Cd, Cr, Cu, Mn, Ni, Pb, V and Zn in solid layers from pits excavated at a redundant industrial site. The work highlighted the importance of analysing samples from across a site and at different depths when assessing the extent of metal contamination on industrial land. Geochemical analyses of dated ombrotrophic peat cores from the Strohner Marchen and nearby Durre Maar, Eifel, Germany, were undertaken by Kempter and Frenzel³⁰⁸ to identify the impact of the long local history of land reclamation and exploitation going back to the Neolithic period.

A paper by Lambert et al. 309 considered the measures taken by a pharmaceutical company to ensure compliance with legislation on environmental occupational health, describing a continuous sampling system installed on a hazardous waste incinerator. Dhir et al. 310 studied the chemical profiles of cement pastes exposed to a chloride solution spray using both XRF and thermogravimetric (TG) techniques. Cooper et al. 311 described a feasibility study for using a continuous extractive filtration sampling system with off-line XRF analysis to demonstrate hazardous element emission compliance at an American Environment Protection Agency (EPA) test incinerator. The authors were working towards 'at-stack' applications with reporting times of the order of 5 min. Mass concentrations and elemental composition of PM_{10} in class-rooms were published by Janssen *et al.*³¹² Measurements were conducted in two schools and outdoors in Amsterdam, The Netherlands, and the elements determined included Br, Ca, Cl, Pb, S, Si and Ti.

A recurring theme during this review period has been the number of workers who use more than one technique to satisfy the analytical demands of *environmental analysis*. A more comprehensive review of all techniques used can be found in our sister ASU review written by Cave *et al.*³¹³

9.5 Archaeological and forensic

Particularly because of its non-destructive capabilities, XRF continues to be applied widely in archaeological applications. As in previous years, a significant contribution has been made by XRF in the analysis of *ancient pottery, ceramics and porcelain*. In this application, Hall *et al.*³¹⁴ advocated EDXRF to determine the minor and trace element composition of ceramic ware and clays from the Egiin Gol valley in Northern Mongolia. Using PCA and bivariate kernel density estimates on the data, it was suggested that there were 5 distinct sources of raw material used to manufacture pottery. Similarly Punyadeera *et al.* 315 used WDXRF to analyse pottery fragments from the Mngeni river area in S. Africa in a provenance study of Iron Age pottery. In another pottery provenance application, Adan-Bayewitz et al. 316 reported a recently developed high-precision XRF method for the determination of 13 trace and 4 major elements in pottery samples. The paper included a comparison between XRF data and results by INAA, indicating the advantages of the former. The effectiveness of their method was demonstrated by its ability to distinguish the products of two closely situated pottery manufacturers in Roman Galilee, which could not be clearly differentiated by INAA. The use of XRF for the analysis of ancient pottery and ceramics to examine the possibility of predicting prehistoric cultural exchanges was the subject of a paper by Pillay *et al.*³¹⁷ In a contribution from a Chinese institution, Yu and Miao³¹⁸ employed EDXRF to measure the Fe: Mn ratio of porcelains originating from several time periods. This ratio was found to be suitable for fingerprinting porcelains from the different eras and was also able to confirm that most imperial-ware blue and white porcelains of the Xuande period used imported material

containing Co and that these artefacts had lower Mn and higher Fe content when compared with those with native material. The ratio was also beneficial in the identification of fakes. To conclude this topic, a study of the use of XRF in the provenance and dating of ancient Chinese porcelain was presented by Leung and Luo. 319

The analysis of *metal artefacts and coins* is another area where XRF has been extensively utilized. Demortier *et al.*³²⁰ discussed the complementary use of radioisotope-excited XRF, PIXE and gamma-ray absorption spectrometry for the surface and bulk examination of valuable and delicate gold jewellery. Using the Lachance–Traill correction model with theoretical α -coefficients, Mao³²¹ determined the Cu, Pb and Sn content of ancient bronze coins, whilst in another coin application Al-Kofahi and Al-Tarawneh³²² examined seven ancient dirhams from the Ayyubid period (1167-1248 AD) and nine from the Mamluk period (1248–1459 AD) of the Great Islamic Empire. The Ayyubid dirhams were found to contain between 8 and 52% m/m Ag compared with 12–55% m/m for the Mamluk. Copper (5–79% m/m), Au (600 μ g g⁻¹–15% m/m) and Pb (1– 9% m/m) were also found and, rather surprisingly, Hg was present at up to 30% m/m in the Ayyubid coins, whereas a high of only 0.4% m/m was noted for the Mamluk. Other elements found in varying concentrations included Al, Br, Ca, Co, Cr, Fe, Mg, Ni, Rb, S, Sb, Si, Sm, Sr and Ti. The silver content was compared with that of other dirhams from the Umayyad (702– 748 AD) and Abbasid (779-815 AD) periods and the correlation between the various compositions and their historical significance was discussed. Two variants of X-ray spectral analysis were used by Klockenkämper et al. 323 to study near-surface silver enrichment in 218 Roman Imperial silver coins. Electron-beam excitation and EDS was used for the analysis of the uppermost thin layer of each coin whilst WDXRF was used for the analysis of thicker layers. Silver and Cu as majors and 18 minor elements were determined quantitatively. By comparing the Ag content of both sides of a coin, inhomogeneities could be identified. Comparison of the Ag content of the upper thin and the thick surface layers permitted the detection of near-surface enrichment.

The non-destructive capabilities of XRF have no better use than in the investigation of paintings and other works of art. Identification and quantification of the elements in objects of archaeological interest provide information on the origin of the raw materials and the technology involved in their production. Several papers discussed the relevance of XRF and other new analytical techniques for the investigation of archaeological artefacts and works of art. That by Mantler and Schreiner³²⁴ presented examples which included pigments in paint layers and illuminated manuscripts, iridescent glasses and medieval coins, whilst Aloupi et al. 325 considered Bronze Age wall paintings from Knossos, Thera, Pylos, Tiryns and Mycenae. This paper also reported the use of XRD to complement elemental results by XRF and obtain information relating to the mineralogical composition. As an example, the blue pigments were identified to be either natural glaucophane, Na₂(Mg,Fe)₃Al₂Si₈O₂₂(OH)₂, (a member of the amphibole group) or synthetic Egyptian blue CaCuSi₄O₁₀.

Several authors described the *use of mobile XRF spectrometers* in the study of works of art, suggesting that this may be the trend for future work. In this area Leutenegger *et al.* ³²⁶ reported on the realization of a high resolution XRF spectrometer utilizing a Peltier-cooled silicon drift detector. This system was capable of achieving energy resolutions better than 150 eV FWHM at 5.9 keV and was used to investigate different kinds of works of art, paintings and metal alloys. In a study of the artistic and cultural patrimony of the Valencian community in Spain, Ferrero *et al.* ³²⁷ applied XRF technology to the *in situ* examination of works of art, which included paintings, silver ornaments and the ink and paper of manuscripts and engravings. In a more specific application, the same authors ³²⁸

described an XRF system which used two detectors [Si(Li) and CdZnTel for the non-destructive analysis of the inorganic elements which constituted the yellow pigment found in fifteenth and sixteenth century altar pieces painted by a number of Valencian artists. From results obtained it was possible to demonstrate the influence of elements and pictorial techniques of European art on the region of Valencia. A paper by Neelmeijer et al. 329 listed the requirements of modern analytical techniques in the analysis of pigments in paintings. In particular, it was shown that XRF and PIXE methods could be used in a complementary manner. The ion beam techniques of external PIXE plus Rutherford backscattering could distinguish the painting technique (for example paint layer arrangements and pigment admixtures), whilst portable XRF was purported to be a valuable tool for pre-selecting areas of interest which could then be transported to the ion beam laboratory. The possibility of distinguishing between two or three layers of paint was reported, but it was difficult to interpret more complex paint layer types. A joint venture to study the use of XRF and INAA for the examination of works of art was reported by Panczyk et al. 330 The group had interests which included panel paintings, Chinese and Thai porcelain and the contents of Egyptian sarcophagi.

XRF was one of the techniques employed by several authors for the mostly non-destructive analysis of *ancient glass*. Hoffmann *et al.*³³¹ were concerned with coloured glass beads of the Merovingian period recovered from female graves at burial sites in the Black Forest, Germany. Ornamental Celtic glasses were studied by Wobrauschek *et al.*, ³³² whilst the interest of Smit *et al.*³³³ was in 16th century Slovenian glasses.

9.6 Industrial

As has become the norm, a significant contribution to this section is in the field of metal and alloy analysis with the iron and steel industry accounting for approximately half. With the fairly recent advent of analyser crystals for light elements, the paper by Guo et al. 334 describing the analysis of carbon in low alloy steel is of particular interest. The sample, after polishing, was measured at a vacuum of 6 Pa, with the tube operated at 40 kV and 70 mA and a count time of 60 s. A calibration graph was obtained which was linear to 1% m/m C with a detection limit of 0.018% m/m. No significant interferences were present when the C Kα line was used. Criteria for selection of grinding media were also discussed. Phosphorus in high phosphorus cast iron was the subject of interest for Cai and colleagues³³⁵ at the Ministry of Railways, Changzhou, China. The sample (2.4 g) was ground to 300 mesh and compacted with a methylcellulose binder (5:1) in a hard 25 mm plastic ring using a pressure of 30 kN. The resultant disc was analysed by EDXRF using Fe Kα as an internal standard and the multifunctional Lucas-Tooth intensity correction software. Calibration linearity from 1.65 to 6.05% m/m of P was reported using the P K α line, with results obtained to a precision of 1.6–2.2% RSD. In another Chinese application, Hao $et\ al.^{336}$ reported the use of XRF to measure Al, Cr, Cu, Mn, Ni, P, S, Si, Sn, Ti and Zr directly on silicon-steel chips, whilst in a Russian report, Kalinin and Plotnikov³³⁷ examined the suitability of XRF for determining elements between Sc and U in steels and copper and nickel alloys. Dénes *et al.* ³³⁸ reported the use of EDXRF and XRD techniques in a study to determine parameters influencing the adhesion of oxide layers during the oxidizing processes of steels. Technical difficulties prevent much experimental work from being undertaken under industrial conditions, so the study included findings from laboratory simulations. It was shown that silicon had a major effect on the removability of the oxide layers. Finally, Dobson *et al.*³³⁹ reviewed the requirements of a new generation of laboratory automation systems in the iron and steel industry with particular reference to the benefits achieved at various world-wide user sites.

Two references were pertinent to *precious metals*. That by Stankiewicz and colleagues³⁴⁰ at the Institute of Non-ferrous Metals, Gliwice, Poland, described a method for the production of certified gold reference materials for utilization in a non-destructive XRF spectrometry method, whilst Savolainen *et al.*³⁴¹ proposed the use of XRF for the preliminary assaying of precious metals prior to selection of optimal analytical procedures.

Alloys were the subject of interest for several Chinese publications, including that of Wang et al., 342 who reported a method (including the preparation of reference materials) for the analysis of the Ni and Ti content of nickel-titanium memory alloys. The use of XRF to check the homogeneity of zinc based alloys, with reference to levels of Ca, Cd, Fe, Pb and Zn, was proposed by Fan et al. 343 Finally, in this section, an Indian contribution by Joseph and Sharma 344 reported the use of EDXRF for the elemental analysis of Cu–Ni alloys, Nd aluminide and Fe and Ni powders. A 109 Cd radioisotope source was used to analyse all materials except the Nd–Al alloy, where a 241 Am source was used. The rapidity of the analysis was stated to be a significant aid in controlling the composition of the charge constituents for the Cu–Ni alloy and it was also noted that, for the metal powders, there was appreciably heavier contamination of Fe in the Ni than vice versa.

Once again a major contribution has been made in the field of ores and other chemical products. A simple method was proposed by Wang et al. 345 for the analysis of tungsten ores. A glass disc was prepared by mixing 80-100 mg of dried, powdered sample, 3.4 g of Na₂B₄O₇, 2.8 g of Li₂B₄O₇ and 250 mg of NaNO₃ and fusing at 1050-1100 °C for 6-8 min, with a further fusion for 4-6 min with 20-30 mg KI as a releasing agent. An RSD for the WO3 at 60-70% m/m was claimed to be <1% and was stated to be comparable with gravimetric methods. Zhao and Wang³⁴⁶ advocated a fusion process for copper sulfide ores which utilized 250 mg of dried, powdered ore pre-oxidized with 1 g of NaNO₃, 6 g of a 12:22 mixed fusion agent (Li₂B₄O₇–LiBO₂) and 200 mg of SiO₂ to facilitate glassing. Xu and Liu ³⁴⁷ presented fusion conditions for the analysis of iron ores in which the sample (0.4 g) was fused with 4 g of anhydrous $\text{Li}_2\text{B}_4\text{O}_7$, 0.5 ml of 400 g l⁻¹ HNO₃ and 0.4 ml of 20 g l⁻¹ NH₄I. It would be unusual to see the high flux to sample ratios used in some of this work coupled with the generous use of releasing agent employed in Western laboratories. Willis and McNew³⁴⁸ at the University of Cape Town, South Africa, produced an extensive evaluation of the problems faced in the analysis of monazite and REE compounds by WDXRF. Aspects considered were infinite thickness, line overlaps, crossing of major element absorption edges, lack of reference materials and inadequacies in most influence coefficient software to handle up to 32 elements in a single run. This appears to be a very useful guide to those entering the field of multielement REE analysis for the first time. EDXRF was utilized by Budak et al. 349 for the analysis of Ba, I, In, Mo, Sb, Sn and Sr in ores from the Mazi mountain town of Mardin, Turkey, and also by the same authors³⁵⁰ to measure the Ba, Cu, Fe, I, In, Sb, Sn, Sr and Zr content of malachite ore from the Narman region in the city of Erzurum, Turkey. The analysis of Nb-Ta ores by EDXRF was carried out by Funtua.³⁵¹ The analysis of samples from the alkaline granite province and central pegmatites of Nigeria was performed by utilizing a Mo secondary target for Fe, Mn, Nb and Ta as majors and Co, Hf, Pb, Rb, Ti, Th, U, W, Y, Zn and Zr as additional constituents. The final contribution to the analysis of ores concerned the preparation of calibration samples to mimic the matrix of ilmenite ore. Wongnawa et ³² showed that XRF spectra recorded at three positions on samples pelletized with corn starch (1:5) gave lower baselines than from synthetic calibration samples due mainly to the contribution of Compton scattering. A method to overcome this effect by adding extra amounts of the major elements to the

the calibration samples was proposed with supporting validation data.

The analysis of other chemical materials included work by Zhuo et al.,353 who proposed a fusion method for the determination of K₂O and Nb₂O₅ in lithium potassium niobate, involving 0.15 or 0.4 g of sample, 6.8 g of a 6:11 mixture of lithium tetraborate and lithium metaborate and 0.2 g of silica, and Asakura et al.³⁵⁴ who reported a fusion method to determine the fluorine content of calcium silicate/ fluoride composite materials. In this latter work, it was possible to obtain a transparent glass bead by melting a 1:1 flux (LiBO₂) to sample mixture at 780 °C for 10 min, and a precision of 0.154% RSD could be obtained when preparing samples containing artificial cryolite. Theoretical matrix coefficients were calculated and it was noted that overlap corrections for Fe Lα and Mn Lα were necessary. The method showed good precision with an RSD of 0.017% and it was possible to measure the fluorine content from 0.2-12% m/m in a range of different calcium silicate fluoride composites.

The contribution made by the cement and allied industries has dwindled over the last few years due to the development of well established methods where any new degree of novelty is difficult to achieve. This year has probably produced an alltime low with all but one paper related to instrument manufacturers. Since it is not the intention of this reviewer to extol the virtues of or favour any one particular manufacturer these references are simply listed so that they can be examined more fully at the reader's whim: Ji et al.³ concerning an EDXRF configured with a low power Cu anode tube; Kern and Uhlig³⁵⁶ with a review of modern X-ray instruments; and finally Anon.³⁵⁷ who considered XRF equipment for cement plant process control. The one nonmanufacturer-related contribution concerned the preparation of reference samples for the XRF analysis of cement powders, where Iordanov et al. 358 described methodology to develop a set of reference materials using samples analysed against synthetic standards, presumably prepared from high purity oxides.

XRF appears to be developing an increasing impact in the oils, lubricants and fuels industries, judging by the number of abstracts reviewed this year. The analysis of low levels of sulfur in fuel oils has always been an area of interest and the first three papers continue that interest. Bettinelli et al. 359 used data provided by standard XRF methods (ASTM D4294-90 and ASTM 2622-94) to evaluate the accuracy of results obtained by a high temperature method (ASTM D1552-90). Although EDXRF has been accepted as the preferred method for the determination of S in fuels, it has not been well evaluated below $100 \,\mu g \, g^{-1}$. The report by Pessayre et al. 360 evaluated the reproducibility and repeatability and the influence of the C/H ratio for low S diesel oils. Using the sample mounted on a Mylar-backed aluminium ring, Njue et al. 361 used EDXRF to analyse the S content, together with As, Cu, Fe, Hg and Pb, of waste engine oils collected from garages in and around Nairobi. Typical values were reported and comparison with AAS demonstrated. A method for improving inter-element factors in the determination of additive and trace elements in lubricants was put forward by Van Driessche and Sieber. 362

A closely related application, although determinations are undertaken for different reasons, is the analysis for the evaluation of *engine or machinery wear*. Several publications in this very important sphere have been reviewed. Although oil filters can contain useful information relating to wear mechanism, filter analysis for wear detection is very rarely performed due to the method being very cumbersome. However, the oil itself can obviously be analysed very economically. Using a small passenger car diesel engine as a test tool, Toersen and Slob³⁶³ compared the results of filter analysis with those simultaneously performed on the oil after changes at each 10 000 km interval up to the expected life of the

engine at 165 000 km. Trends were different for the two analysis types, prompting the authors to suggest the design of dedicated diagnostic filters for wear debris detection. Methodology for applying EDXRF analysis to the F404 engine onboard the F-18 weapon system was developed by Humphrey. This method enabled over 100 h of advance warning of engine failure. EDXRF was chosen over AES because of its ability to analyse particles larger than 10 µm with no alteration of their chemical form. A review was produced by Whitlock samining X-ray related techniques used to study or monitor the wear condition of naval machinery, whilst with coauthors he outlined the advantages of analysing and monitoring filter debris over the analysis of particulates suspended in oil.

Nuclear related applications have made a significant impact during the current review period, perhaps suggesting another area where XRF is coming to the forefront as the preferred method. As part of a co-operative program between the USA and Russia to improve systems of nuclear material protection, control and accountability, Ryon and Ruhter³⁶⁷ developed methodology for the assay of Pu and U solutions. A ⁵⁷Co source was used to excite the element K lines and a mixed ⁵⁷Co plus 153Gd transmission source was utilized to correct for absorption variations. This feature was unique since it allowed accurate calibration with a single standard solution and a wide concentration range (up to 300 g l⁻¹). Research carried out in the use of X-ray and low energy γ -ray spectroscopy for the measurement of actinide concentration in the re-processing of highly active waste was presented in two references by Howarth et al. 368,369 Elemental impurities in uranium oxide were measured by Parus et al. 370 using WDXRF, and finally a study on the use of multi-techniques (inclusive of WDXRF) for the qualitative and quantitative analysis of materials considered to be signatures for nuclear proliferation was reported by Swartz.371

To end, a few *miscellaneous applications*, once again show the diversity and usefulness of XRF as an analytical tool. A comparative study on the use of XRF, ICP-AES, ICP-MS and AAS in the analysis of scrap electrical devices was presented by Cuhls *et al.*, ³⁷² whilst a contribution in Japanese by Amano and Nishikata³⁷³ supported the use of X-ray detection for the measurement of poly(vinyl chloride) in waste plastics. In the field of study of the effect of detergents on textile, van Dalen³⁷⁴ developed a methodology to measure the iron content of cloth without resorting to sample pre-treatment. A patent application was proposed by Thebock *at al.* ³⁷⁵ for the use of X-ray spectroscopy to detect the coating (composed of two or more substances) applied to an article to act as a bar code identifier. Finally, Wehausen *et al.* ²⁹⁷ compared XRF with other common analytical methods for the determination of the major and minor element content of brine solutions.

9.7 Clinical and biological

XRF continues to make a vigorous contribution to in vivo studies, particularly in the measurement of lead in bone, as judged by the healthy crop of publications that have appeared during the current review period. For example, McNeill et al. 376 reviewed the use of the two categories of instrumentation in regular use, radioisotope source-based systems and polarized systems that incorporate an X-ray tube source. To illustrate the radioisotope source instrumentation, the measurement of Pb and U in bone was discussed. To illustrate polarized in vivo XRF, the determination of Cd and Hg in kidney samples was discussed as these applications represent both existing and new developments. In vivo measurement of Pb by XRF was also described by Lee³⁷⁷ as the biological monitoring stage of a comprehensive programme for measuring and controlling the occupational exposure to Pb of workers in Korea. This biological monitoring stage was considered to be very useful

in identifying and reducing excess lead absorption in the circumstances of a developing country where engineering controls could not be introduced sufficiently quickly. A further review of the capabilities of *in vivo* XRF was presented by Bradley and Farquharson,³⁷⁸ who highlighted the use of the technique in occupational exposure and the monitoring of heavy metal exposure, but more particularly in the in vivo determination of iron in skin as a contribution to the study of the hereditary disorder, β-thalassema, which results in a buildup of Fe in body tissue. Preliminary results using a tungsten tube excitation source in which the primary beam was both collimated and filtered using a Cu foil as a K-edge filter showed that the resultant 8.4 keV W excitation could be used to detect levels of less than $10 \ \mu g \ g^{-1}$ in skin tissue using a $1000 \ s$ count time and imparting an entrance surface dose-rate of a few mGy min⁻¹. Farquharson and Bradley³⁷⁹ complemented this study with a paper in which they gave more details of the instrumentation used for the evaluation of Fe in skin at low patient radiation dose.

Further work has also been published in evaluating and improving the in vivo technique. Bradley et al., 380 in another contribution from the University of Malaya, investigated the contribution of Pb to the total elastic scatter intensity using a computer simulation for Pb concentrations in the range 0- $1000 \, \mu g \, g^{-1}$ in bone. Their results indicated that this contribution increased sharply above the Pb photoelectric effect threshold (100 keV), calling into question the reliability of using the elastic scatter peak as a normalizing factor for the quantity of bone in in vivo applications. Szaloki et al.381 investigated the fundamental parameter method for the in vivo XRF determination of Pt, in the concentration range from 25 to 1000 μg g⁻¹, based on an investigation of the response from phantoms that simulated the use of Pt-based chemotherapeutic drugs in head and neck tumours. Average differences between nominal and measured results were <8% for phantoms in air (representing Pt in superficial sites) and <15-20% when immersed in water to simulate greater depths of overlying tissue. Although not strictly an XRF application, Speller³⁸² investigated the information content of both coherent and incoherent scattering in the X-ray analysis of tissue with particular relevance to the study of osteoporosis and breast cancer. Although the opposite of an *in vivo* study, it is nevertheless relevant to note the work of Aro *et al.*, ³⁸³ who evaluated the performance of Pb determinations by K-line XRF by the analysis of cadaver legs. The aim of this study was to validate the in vivo bone Pb technique on samples where confirmatory analyses could be obtained directly on the bone instead of relying on phantoms. Close agreement with independent analyses of bone by ICP-MS was obtained.

Monte Carlo simulations, designed to optimize in vivo measurements, has featured in several publications during the current review period. Ao et al. 384 used this simulation technique to evaluate sources of error in K- and L-line techniques for the determination of Pb. Results showed that the thickness of overlying soft tissue, distance of analyser from bone sample, distribution of lead in bone, and bone dimensions, all affected the accuracy of results and that the method of ratioing Ka X-ray intensity to the intensity of the coherent scatter peak from the excitation source minimized most measurement errors and significantly improved accuracy (but note the study of Bradley et al., 380 summarized above, which indicates that the scatter peak intensity is affected by Pb concentration). Employing the L-line XRF method, use of Pb Lα and Lβ to measure Pb concentration and skin thickness simultaneously minimized the effect of skin thickness on Pb results and was found to offer greater sensitivity. In a second contribution, Ao et al. 385 employed a Monte Carlo-library least squares approach to improve measurement accuracy in the determination of Pb in bone using both the K- and L-line XRF approach and reported reductions in the relative standard

deviation of 3–20 times for a prototype 109 Cd-based K-line XRF instrument and 1.4–3 for a polarized X-ray tube L-line instrument. Monte Carlo simulation was also used by Fayez⁶⁰ to develop a 90° geometry polarized XRF system to measure Cd in deep body organs (*e.g.*, the kidney). Results showed that 4–30 μ g g⁻¹ Cd could be detected for distances of skin to kidney of 30–70 mm, respectively, delivering a mean dose of 9 mGy to the skin.

Considering now clinical studies related to Pb exposure, Gerhardsson et al. 386 described an investigation to discover whether lead in bone is available for chelation by meso-2,3dimercaptosuccinic acid (DMSA). Urine and blood samples from secondary lead smelting workers were analysed by AAS and ICP-MS techniques, and compared with in vivo finger bone Pb by K-XRF. Their conclusion was that DMSA-chelatable Pb largely reflects the concentration in blood, soft tissues and possible trabecular bone, but for an estimate of total bodyburden and long term exposure, estimation of cortical bone lead is necessary. The well known effect of lead exposure from drinking water was investigated in the city of Boston, where older houses contain lead plumbing, by Potula and colleagues.³⁸⁷ Using 1976–1977 data on Pb in the tap water of homes and more recent data on blood and tibia/patella Pb contents measured by K-XRF, a correlation was found between patella Pb levels and subjects living in houses with lead levels of 50 μg l⁻¹ (first morning tap water) and it was concluded that Pb-contaminated tap water was an important predictor of elevated bone lead levels later in life. Rosen³⁸⁸ undertook a clinical study by L-line XRF in children, teenagers and adults from lead exposed and non-lead-exposed suburban communities in the US to provide new epidemiological information of relevance to hypertension, osteoporosis and the effect of maternal Pb to the developing foetus. The so-called 'O'Flaherty model', which is a physiologically based computer simulation of Pb deposition in humans, is well suited to comparisons with non-invasive bone Pb measurements made by XRF, and was evaluated by Fleming et al. 389 Good agreement was found between the model and observations on a lead smelter population and further refinements to the model were suggested.

Teeth and hair have always been relatively accessible samples for clinical studies and Zaichick et al. 390 described a 109 Cd EDXRF facility for the *in vivo* determination of Ca, Pb, Sr and Zn in tooth enamel. The instrument design irradiates only a small part of the tooth, minimizing doses to the face and mouth cavity. Calibration was achieved by comparative INAA analysis and the Ca content of tooth enamel was suggested as an internal standard for *in vivo* EDXRF. By contrast, Leung et al. 391 determined Ca, Fe and Zn in the hair of 93 pregnant women in China who were judged on the basis of blood serum indices to have deficiencies in these elements. The women were given dietary supplements and the hair analyses were observed to follow this supplementation.

Considering now other clinical studies, EDXRF was used by Zaichick and Zaichick³⁹² to determine iodine in thyroid puncture biopsy specimens collected to provide pre-surgical diagnostics on benign and malignant nodules. Muramatsu et al.³⁹³ measured the distribution of Th in selected organs in autopsy samples from Thorotrast patients and identified thorium conglomerates as part of a wider study to determine the concentration of Th in these organs by ICP-MS. In a rather different kind of application, Halmagean et al.³⁹⁴ used a Si-PIN detector to measure the spectral distribution of back-scattered X-ray radiation observed during *in vivo* angiography procedures. The aim was to evaluate the risk of exposure to medical staff and devise suitable shielding, though no doubt some of the detected radiation originated from the fluorescence effect. Finally, Forslind³⁹⁵ presented a historically-based review of biomedical applications of particle probes and X-ray analysis emphasising the advantages resulting from newly developed

XRF techniques that offer high sensitivity. A full picture of applications in this area can be found in the current companion ASU review of Clinical and biological materials, foods and beverages presented by Taylor *et al.* ³⁹⁶

In terms of *studies on aquatic species*, the muscles and livers of rainbow trout were analysed by Akyuz *et al.*³⁹⁷ by radioisotope EDXRF and INAA for a range of elements to determine differences in composition between farm cultivated fish and river fish. Farmed fish were found to have a higher Fe content. Demospongiae (sponges) from the eastern Atlantic coastal waters were analysed for a range of elements using EDXRF by Araujo *et al.*³⁹⁸ Silicon was found to be the dominant element, as expected, but different species selectively concentrated Ni and Zn in a manner unrelated to sampling location and high levels of Br were found, particularly in sponges that were low in Si.

XRF has contributed to a range of studies of plant materials over the current review period. A rapid EDXRF method for the determination of Ca, Cl and K in leaves from barley was described by Miah et al. 399 using instrumentation that selectively excited an area of <100 μm. Samples were taken from plants grown on land that had been fertilized chemically and with different combinations of sewage sludge and the study was designed to provide information on the nutritional status. The same group⁴⁰⁰ described similar aspects to this study with particular emphasis on K-deficient plants. Bao et al. 401 described an XRF method for the analysis of fruit juice and found a good correlation with data produced by ICP-AES, and extended this study to muskmelon. 402 A range of Indian spices were analysed by Joseph et al. 403 using a radioisotope EDXRF technique and the implications for toxicity and significance with respect to the human diet were discussed. The same category of instrumentation was used by Harangozo *et al.* 404 to measure the Fe and Zn content of a range of plants having medicinal properties and by Ivanova et al. 405 to analyse plant materials and soils, with validation by the analysis of suitable reference materials. The capabilities of a range of instrumental techniques (INAA, EDXRF, ICP-AES and AAS) were evaluated by Djingova *et al.*⁴⁰⁶ through the analysis of various plant reference materials. A combination of INAA and ETAAS was recommended where the application was monitoring environmental pollution. The same group 405 undertook EDXRF measurements on heavy and toxic metals in plants and soils, presenting details of the analytical procedure and comparing results favourably with determinations by INAA and AAS.

9.8 Thin films

The ability of XRF to satisfy the analytical needs of the semiconductor manufacturing industry continued to feature in the literature during this review period. The thin layer characterization of (Ba, Sr)TiO3 (BST) thin films was studied by Bogert et al. 407 to assist in the development of capacitors for ultra-large scale integrated dynamic random access memories (ULSI-DRAMS). Energy dispersive XRF was used to determine thin film composition and thickness measurements within $\pm 2\%$ with an analysis time of ~ 8 min. Kurt et al.⁴ investigated the effect of doping on the thermoelectric properties of iridium silicide thin films. Accurate control of B and P concentrations in borophosphosilicate glass (BPSG) films deposited by chemical vapour deposition (CVD) was reported by Goyal and Westphal. Stringent requirements set by semiconductor technology were met by Jurczyk et al. 410 in their determination of Co, Cr, Cu, Ga, Ni, Sb, Se, Yb and Zn in microsamples of semiconductor type multi-element materials using the thin layer method. Eisgruber et al. 411 demonstrated how CuIn_xGa_{1-x}Se₂ (CIGS) module fabrication was improved through the use of XRF as an in situ composition monitor.

A semi-empirical derivation of thin film sensitivities for

EDXRF spectrometers was published by Kellogg. 412 This mathematical approach provided sensitivities for elements for which no reliable standards were available and also improved the calibration for those analytes that do have standards. The method was limited to K-line radiation and silicon semiconductor detector EDXRF systems with secondary or monochromatic excitation. A two-step approach towards model-free XRF analysis of layered materials was offered by Dane $et\ al.$ A generic algorithm was first used to obtain the number of layers and estimate element concentrations and thickness of each layer, followed by a gradient technique to refine the estimation. A study of carbon films on silicon wafers was reported by Kataoka *et al.* 414 Their method for the calculation of characteristic X-ray intensity of thin films included the effect of secondary excitation by photoelectrons and Auger electrons. The actual intensity calculation was reported to be finished in seconds by using the tabulated results of a Monte Carlo simulation. Mantler⁴¹⁵ also used Monte Carlo techniques for the qualitative analysis of thin films and multiple film structures.

A procedure for the *determination of thickness* of Ag and Au films and foils coated on a metallic Cu foil substrate was described by Ekinci *et al.*⁴¹⁶ Neumaier⁴¹⁷ introduced a practical method for measuring the thickness of Zn₃(PO₄)₂ coatings on steel surfaces. Layer thickness and composition of Al₂O₃–Ti(C,N) materials were studied by Rossiger⁴¹⁸ in a German language publication.

Other applications included work by Klenk et al. 419 on measurements of thin film chalcopyrite solar cells. Diffusion of O and P and segregation in nickel was studied by Schulze et al. 420 using an ultra-high vacuum system. A comparison of X-ray analytical methods was published by Ebel et al. 421 for the investigation of thin layers by XRF, EPMA, XPS and total electron yield (TEY). The same group 422 at the Technical University of Vienna, Austria, also published an application for the detection of submonolayers. Ashour et al. 423 characterized grafted polypropylene sheets doped with different metals, such as Co, Cu, Fe and Ni. A new method of preparing microsamples of mono- and poly-crystals and of silicate rocks was published by Jurczyk et al. 424 The chemical compositions of serpentine, nepheline, syenite, basalt and shale for Co, Cr, Cu, Fe, Ga, Mn, Ni, Se, V and Zn were reported.

9.9 Chemical state analysis and speciation

Chemical shift and the line shape of XRF spectra have been studied by a number of workers to establish different chemical states of first row transition element compounds. Konishi et al. 425 published studies on 32 materials containing Ni. The intensity ratios of $2p_{3/2}$ to $2p_{1/2}$ deconvoluted spectra of K_2CrO_4 and $KMnO_4$ were reported by Oku *et al.* 426 Raj *et* al. 427 considered the influence of alloying effects on K β /K α Xray intensity ratios of Ni and V in $V_x Ni_{1-x}$ alloys. The same group at the Institute of Physics, Bhubaneswar, India, 428 also studied valence electron structures of Co, Cr, Ti and V in selected silicide compounds. Kucukonder *et al.* 429 used a ²⁴¹Am source to excite their samples and measured the K spectra using Si(Li) and Ge(Li) detectors. The Kβ/Kα intensity ratios were calculated using Brunner's model and were found to be in good agreement with previously published experimental data. A study of ligand (N,O,F) 2s to metal Mn 1s interactions was reported by Bergmann *et al.*⁴³⁰ The energy of the K β " feature was related to the ligand 2s binding energy and was used to identify the type of ligand. Spin state analysis of epitaxial Mn compound films was investigated by Yamaguchi et al. 431 using high resolution XRF spectra. A high resolution configuration was also used by Anagnostopoulos et al. 432 to study metallic Sc. Deviations in the $K\beta/K\alpha$ intensity ratio of Ti upon impact with low velocity ions were reported by Wijsman and Vis.⁴ The Dirac-Fock method was used by Mukoyama et al. 434 to

perform relativistic calculations of the K X-ray transition energies of Ti atoms with various electron valence shell configurations.

The K X-ray satellite spectra of Ca in CaCO₃ and CaHPO₄·2H₂O excited by photons were reported by Murti et al. Torok et al. published work on a new and comprehensive compilation of experimental values for K satellite and K hypersatellite energy shifts. The $K\alpha_2^h$ hypersatellite spectrum of chlorine was studied by Soni salso published work on the KL²-L²V spectrum of silicon. A theoretical intensity distribution analysis of $K\alpha$ satellites emitted from Al, Cl, and K was reported by Yamamoto et al. 439

The chemical effects on the L X-ray spectra of Ba, Ce and La compounds were investigated by Baydas $et~al.^{440}$ Amstrong⁴⁴¹ advised on the pitfalls and promises in the determination of the chemical valence state of transition elements (Sc to As), measured from variations in intensity ratios of L α and L β lines in metal alloys. The use of the Mn L α line to study chemical effects in X-ray analysis and probe sample homogeneity was reported by Lawniczak-Joblonska et~al., ⁴⁴² who examined the Mn content of semi-magnetic conductors and epitaxially grown layers.

Other applications included calculations of X-ray emission spectra for sulfur dioxide by the DV-Xa method, published by Song et al., 443 and a novel X-ray absorption near edge structure (XANES) method using WDXRF, which was published in a Japanese language paper by Kawai et al., 444 who measured the X-ray emission fine structure of Si.

A procedure was developed by Latva *et al.*⁴⁴⁵ for speciation studies of As in aqueous solution. The separation and independent EDXRF determination of microgram quantities of As^{III}, As^V, dimethylarsinic acid and phenylarsonic acid were collected one by one from the same solution by absorbing them onto metal-loaded activated charcoal. The detection limits reported for all four As species were better than 0.02 mg l⁻¹.

References

- P. Wobrauschek, P. Kregsamer and M. Mantler, X-ray Fluorescence Analysis, *Instrum. Multi-Elem. Chem.*, Kluwer, Dordrecht, Netherlands, 1998, 302–345.
- I. I. Mirenskaya, N. I. Shevtsov, A. B. Blank and K. N. Belikov, J. Alloys Compd., 1999, 286(1-2), 76.
- A. K. Cheburkin and W. Shotyk, X-Ray Spectrom., 1999, 28(3), 145.
- 4 C. Hombourger, P. Jonnard, J.-M. Andre and J.-P. Chauvineau, X-Ray Spectrom., 1999, 28(3), 163.
- 5 H. Ogata and S. Kitamoto, Astron. Nachr., 1999, 320(4-5), 380.
- 6 U. Bergmann and S. P. Cramer, Proc. SPIE-Int. Soc. Opt. Eng., 1998, 3448(Crystal and Multilayer Optics), 198.
- 7 R. Baskaran and T. S. Selvakumaran, Rev. Sci. Instrum., 1999, 70(6), 2637.
- 8 F. Ullmann, G. Zschornack and H. Tyrroff, Nucl. Instrum. Methods Phys. Res., Sect. B, 2000, 160(2), 290.
- E. Antonucci, L. Ciminiera, A. M. Malvezzi and G. Tondello, *Proc. SPIE-Int. Soc. Opt. Eng.*, 1998, 3443(X-ray and Ultraviolet Spectroscopy and Polarimetry II), 75.
- 10 C. W. Andrus and F. R. Powell, Proc. SPIE-Int. Soc. Opt. Eng., 1998, 3444(X-Ray Optics, Instruments and Missions), 501.
- 11 S. M. Shafroth and J. D. Brownridge, AIP Conf. Proc., 1999, 475(Pt. 2, Appl. Accelerators Res. and Ind.), 1100.
- 12 A. Bassari and S. Gencay, The use of ^{99m}Tc as fluorescing sources in X-ray fluorescence analysis. *Proc. Int. Conf. Phys. Nucl. Sci. Technol.*, American Nuclear Society, IL, USA, 1998, 1613–1618.
- 13 K. Yajima, T. Awata, R. Koizumi, M. Imai, A. Itoh and N. Imanishi, Nucl. Instrum. Methods Phys. Res., Sect. A, 1999, 435(3), 490.
- 14 A. Tartari, E. Casnati, C. Baraldi, C. Bonifazzi and G. Maino, X-Ray Spectrom., 1999, 28, 297.
- R. Schramm, J. Heckel and K. Molt, Adv. X-Ray Anal., 1999, 41, 384.
- S. Uhlig, K. Mauser and G. Granacher, World Cem., 1999, 30(6), 68.
- 17 A. V. Bessarab, S. V. Grigorovitch, V. V. Intyapin,

- V. I. Kundicov, A. V. Kunin and V. A. Tokarev, Rev. Sci. Instrum., 2000, 71(1), 82.
- I. A. Tolokonnikov, At. Energy (N. Y.), 1999, 85(3), 667. 18
- 19 N. Kozul, G. R. Davis, P. Anderson and J. C. Elliott, Meas. Sci. Technol., 1999, 10(3), 252.
- J. F. Dlouhy, D. Mathieu and K. N. Stoev, Adv. X-Ray Anal., 1999, 41, 403.
- K. Shimizu, Jpn. Kokai Tokkyo Koho JP 2000 09,666 (Cl. G01N23/223), 14 Jan 2000, Appl. 1998/176,848, 24 Jun 1998;
- N. Makiishi, A. Yamamoto and H. Maruyama, Jpn. Kokai Tokkyo Koho JP 11 344,455 [99 344,455] (Cl. G01N23/223), 14 Dec 1999, Appl. 1998/154,097, 3 Jun 1998; 8 pp.
- K. Tsuruya, T. Ueda and T. Misawa, Jpn. Kokai Tokkyo Koho JP 11 211,680 [99 211,680] (Cl. G01N23/223), 6 Aug 1999, Appl. 1998/11,279, 23 Jan 1998; 4 pp.
- 24 K. Tsuruya, T. Ueda and K. Misawa, Jpn. Kokai Tokkyo Koho JP 11 211,679 [99 211,679] (Cl. G01N23/223), 6 Aug 1999, Appl. 1998/11,278, 23 Jan 1998; 4 pp.
- H. Kono and S. Kuraoka, Jpn. Kokai Tokkyo Koho JP 11 174,007 [99 174,007] (Cl. G01N23/223), 2 Jul 1999, Appl. 1997/ 272,649, 6 Oct 1997; 9 pp.
- C. Ma, Eur. Pat. Appl. EP 916,940 (Cl. G01N23/22), 19 May 1999, US Appl. 964,615, 5 Nov 1997; 8 pp. 26
- M. Kuwata and K. Saito, Jpn. Kokai Tokkyo Koho JP 11 27 304,734 [99 304,734] (Cl. G01N23/223), 5 Nov 1999, Appl. 1998/ 116,467, 27 Apr 1998; 5 pp.
- C. K. Stahle, D. McCammon and K. D. Irwin, Phys. Today, 28 1999, 52(8, Pt. 1), 32
- D. McCammon, R. Almy, E. Apodaca, S. Deiker, M. Galeazzi, S.-I. Han, A. Lesser, W. Sanders, R. L. Kelley, S. H. Moseley, F. S. Porter, C. K. Stahle and A. E. Szymkowiak, Nucl. Instrum. Methods Phys. Res., Sect. A, 1999, 436(1-2), 205.
- J. Hoehne, M. Altmann, G. Angloher, M. Buehler, F. Feilitzsch, T. Frank, P. Hettl, T. Hertrich, J. Jochum, T. Nussle, S. Pfnur, J. Schnagl and S. Wanninger, Proc. SPIE-Int. Soc. Opt. Eng., 1999, 3743(In-Line Characterization, Yield Reliability, and Failure Analyses in Microelectronic Manufacturing), 162
- S. Wanninger, M. Altmann, G. Angloher, P. Hettl, J. Hohne, J. Jochum, F. Probst, M. L. Sarsa, J. Schnagl, W. Seidel, F. V. Feilitzsch and R. L. Mossbauer, Nucl. Instrum. Methods Phys. Res., Sect. A, 2000, 439(2-3), 662.
- J. Hoehne, M. Altmann, G. Angloher, P. Hettl, J. Jochum, T. Nuessle, S. Pfnuer, J. Schnagl, M. L. Sarsa, S. Waenninger and F. von Feilitzsch, X-Ray Spectrom., 1999, 28(5), 396.
- F. Von Feilitzsch, J. Hohne, J. Jochum and J. Schnagl, PCT Int. Appl. WO 99 54,696 (Cl. G01K17/04) 28 Oct 1999, DE Appl. 19,817,786, 21 Apr 1998, 47 pp.
- J. S. Adams, S. R. Bandler, C. Enss, A. Fleischmann, S. Hunklinger, Y. H. Kim, J. Schonefeld and G. M. Seidel, Physica B: (Amsterdam), 1999, 263, 604.
- A. D. Holland, G. W. Fraser, P. Roth, S. Trowell, E. Gu, R. Hart, P. Brink and S. Guy, Nucl. Instrum. Methods Phys. Res., Sect. A, 1999, 436(1-2), 226.
- 36 K. Mitsuda and R. Kelley, Nucl. Instrum. Methods Phys. Res., Sect. A, 1999, 436(1-2), 212.
- S. Breon, P. Shirron, R. Boyle, E. Canavan, M. DiPirro, A. Serlemitsos, J. Tuttle and P. Whitehouse, Cryogenics, 1999, 39(8), 677.
- C. K. Stahle, R. P. Brekosky, S. B. Dutta, K. C. Gendreau, R. L. Kelley, D. McCammon, R. A. McClanahan, S. H. Moseley, D. B. Mott, F. S. Porter and A. E. Szymkowiak, Nucl. Instrum.
- Methods Phys. Res., Sect. A, 1999, 436(1–2), 218.

 M. D. Audley, K. C. Gendreau, R. L. Kelley, K. A. Arnaud, K. R. Boyce, R. Fujimoto, F. S. Porter, C. K. Stahle and A. E. Szymkowiak, AIP Conf. Proc., 1999, 470[After the Dark Ages: When Galaxies Were Young (The Universe at 2<z<5)],
- M. Kurakado, X-Ray Spectrom., 1999, 28(5), 388.
- P. Hettl, G. Angloher, F. von Feilitzsch, J. Hoehne, J. Jochum, H. Kraus and R. L. Moessbauer, X-Ray Spectrom., 1999, 28(5),
- S. Friedrich, C. A. Mears, B. Niderost, L. J. Hiller, M. Frank, S. E. Labov, A. T. Barfknecht and S. P. Cramer, *Microsc.* Microanal., 1998, 4(6), 616.
- S. Friedrich, L. J. Hiller, M. Frank, J. B. LeGrand, C. A. Mears, B. Niderost, S. E. Labov, A. T. Barfknecht, M. LeGros and S. P. Cramer, J. Electron Spectrosc. Relat. Phenom., 1999, 103(SISI), 891.
- S. Kraft, P. Verhoeve, N. Rando, A. Van Dordrecht, A. Poelaert,

- R. Den Hartog, A. Owens, M. Bavdaz and A. Peacock, Nucl. Instrum. Methods Phys. Res., Sect. A, 1999, 436(1-2), 238.
- S. Kraft, P. Verhoeve, A. Peacock, N. Rando, D. J. Goldie, R. Hart, D. Glowacka, F. Scholze and G. Ulm, J. Appl. Phys., 1999, 86(12), 7189.
- V. A. Andrianov, P. N. Dmitriev, V. P. Koshelets, M. G. Kozin, I. L. Romashkina, S. A. Sergeev and V. S. Shpinel, Physica B: (Amsterdam), 1999, 263, 613.
- A. Castoldi, C. Fiorini, C. Guazzoni, A. Longoni and L. Strueder, X-Ray Spectrom., 1999, 28(5), 312.
- A. Castoldi, E. Gatti, C. Guazzoni, A. Longoni, P. Rehak and L. Struder, Nucl. Instrum. Methods Phys. Res., Sect. A, 2000, **439**(2-3), 519.
- A. Castoldi and C. Guazzoni, IEEE Trans. Electron Devices, 1999, 46(2), 329.
- A. Castoldi, E. Gatti, C. Guazzoni, A. Longoni, P. Rehak and L. Struder, IEEE Nucl. Sci. Symp. Conf. Rec., 1999, 1, 138.
- V. Bonvicini, P. Burger, L. D'Acunto, D. Franck, A. Gregorio, P. Pihet, A. Rashevsky, A. Vacchi, L. Vinogradov and N. Zampa, Nucl. Instrum. Methods Phys. Res., Sect. A, 2000, 439(2-3), 471. J. S. Iwanczyk, B. E. Patt, C. R. Tull, J. D. Segal, C. J. Kenney,
- J. Bradley, B. Hedman and K. O. Hodgson, IEEE Trans. Nucl. Sci., 1999, 46, (3, Pt. 1), 1, 284.
- C. Fiorini, A. Pullia, E. Gatti, A. Longoni and W. Buttler, IEEE Trans. Nucl. Sci., 1999, **46**(3, Pt. 1), 161. C. Fiorini, A. Pullia, P. Novellini, E. Gatti, A. Longoni and
- W. Buttler, IEEE Nucl. Sci. Symp. Conf. Rec. 1998, 1999, 1,
- M. Al-Turany, J. D. Meyer and K. Bethge, Nucl. Instrum. Methods Phys. Res., Sect. B, 1999, 155(1-2), 137.
- K. Sato, Nucl. Instrum. Methods Phys. Res., Sect. A, 1999, 436(1-2), 285.
- N. Ota, T. Marukami, M. Sugizaki, M. Kaneda, T. Tamura, H. Ozawa, T. Kamae, K. Makishima, T. Takahashi, M. Tashiro, Y. Fukazawa, J. Kataoka, K. Yamaoka, S. Kubo, C. Tanihata, Y. Uchiyama, K. Matsuzaki, N. Iyomoto, M. Kokubun, T. Nakazawa, A. Kubota, T. Mizuno, Y. Matsumoto, N. Isobe, Y. Terada, M. Sugiho, T. Onishi, H. Kubo, H. Ikeda, M. Nomachi, T. Ohsugi, M. Muramatsu and H. Akahori, Nucl.
- Instrum. Methods Phys. Res., Sect. A, 1999, 436(1-2), 291. A. V. Golubev, E. G. Pivinskii, V. V. Akulinichev, A. A. Sorokin and S. V. Bobashev, Tech. Phys., 1999, 44(5), 553.
- J. S. Iwanczyk and B. E. Patt, Adv. X-Ray Anal., 1999, 41, 951.
- L. Struder, N. Meidinger, D. Stotter, J. Kemmer, P. Lechner, P. Leutenegger, H. Soltau, F. Eggert, M. Rohde and T. Schulein Microsc, Microanal, 1998, 4(6), 622.
- R. Cesareo, G. E. Gigante and A. Castellano, Nucl. Instrum. Methods Phys. Res., Sect. A, 1999, 428(1), 171.
- S. Barkan, K. F. Ihrig and M. B. Abott, Microsc. Microanal., 1999, 5(2), 120,
- P. J. Statham, *Microsc. Microanal.*, 1998, **4**(6), 605. M. C. Lepy, J. L. Campbell, J. M. Laborie, J. Plagnard, P. Stemmler and W. J. Teesdale, *Nucl. Instrum. Methods Phys.* Res., Sect. A, 1999, 422(1-3), 428.
- B. G. Lowe, Nucl. Instrum. Methods Phys. Res., Sect. A, 2000, **439**(2-3), 247.
- F. Scholze, H. Henneken, P. Kuschnerus, H. Rabus, M. Richter and G. Ulm, Nucl. Instrum. Methods Phys. Res., Sect. A, 2000, **439**(2-3), 208.
- G. Budak, A. Karabulut, O. Simsek and M. Ertugrul, Instrum. Sci. Technol., 1999, 27(5), 357.
- F. Perotti and C. Fiorini, Nucl. Instrum. Methods Phys. Res., Sect. A, 1999, **423**(2–3), 356.
- A. G. Karydas and T. Paradellis, AIP Conf. Proc., 1999, 475(Pt. 2, Appl. Accelerators Res. and Ind.), 858.
- J. T. Walton, M. Amman, G. Conti, W. S. Hong, P. N. Luke and F. P. Ziemba, Mater. Res. Soc. Symp. Proc., 1999, 507(Amorphous and Microcrystalline Silicon Technology-1998), 351.
- B. A. Ludewigt, B. Krieger, D. Lindstrom, M. R. Maier, M. Rutgersson, C. R. Tull and H. Yaver, IEEE Nucl. Sci. Symp. Conf. Rec. 1998, 1999, 1, 365.
- B. A. Ludewigt, B. Krieger, D. Lindstrom, M. R. Maier, M. Rutgersson, C. R. Tull and H. Yaver, IEEE Trans. Nucl. Sci., 1999, 46(4, Pt. 1), 886.
- P. Seller, G. Bale, W. J. F. Gannon, G. Hall, A. D. Holland, G. M. Iles, A. R. Jorden, B. G. Lowe, P. Murray, M. S. Passmore, M. L. Prydderch, K. Smith, S. L. Thomas and R. Wade, *Proc. SPIE-Int. Soc. Opt. Eng.*, 1999, 3774(Detectors for Crystallography and Diffraction Studies at Synchrotron Sources), 30.
- G. Rossi, J. Morse and D. Protic, IEEE Trans. Nucl. Sci., 1999, 46(3, Pt. 1), 765.

- 75 G. Derbyshire, K. C. Cheung, P. Sangsingkeow and S. S. Hasnain, J. Synchrotron Radiat., 1999, 6, (pt. 2), 62.
- A. Keay, A. D. Holland, D. J. Burt and P. Pool, Nucl. Instrum. Methods Phys. Res., Sect. A, 1999, 436(1-2), 16.
- K. Miyaguchi, H. Suzuki, J. Dezaki and K. Yamamoto, Nucl. Instrum. Methods Phys. Res., Sect. A, 1999, 436(1-2), 24.
- H. Soltau, J. Kemmer, N. Meidinger, D. Stotter, L. Struder, J. Trumper, C. v. Zanthier, H. Brauniger, U. Briel, D. Carathanassis, K. Dennerl, S. Engelhard, F. Haberl, R. Hartmann, G. Hartner, D. Hauff, H. Hippmann, P. Holl, E. Kendziorra, N. Krause, P. Lechner, E. Pfeffermann, M. Popp, C. Reppin, H. Seitz, P. Solc, T. Stadlbauer, U. Weber and U. Weichert, Nucl. Instrum. Methods Phys. Res., Sect. A, 2000, 439(2-3), 547.
- P. Fougeres, P. Siffert, M. Hageali, J. M. Koebel and R. Regal, Nucl. Instrum. Methods Phys. Res., Sect. A, 1999, 428(1), 38.
- G. Bale, A. Holland, P. Seller and B.G. Lowe, Nucl. Instrum. Methods Phys. Res., Sect. A, 1999, 436(1-2), 150.
- C. M. Stahle, B. H. Parker, A. M. Parsons, L. M. Barbier, S. D. Barthelmy, N. A. Gehrels, D. M. Palmer, S. J. Snodgrass and J. Tueller, Nucl. Instrum. Methods Phys. Res., Sect. A, 1999, **436**(1–2), 138.
- 82 A. Shor, Y. Eisen and I. Mardor, Nucl. Instrum. Methods Phys. Res., Sect. A, 1999, 426(2-3), 491.
- A. Shor, Y. Eisen and I. Mardor, Nucl. Instrum. Methods Phys. 83 Res., Sect. A, 1999, 428(1), 182.
- 84 T. H. V. T. Dias, AIP Conf. Proc., 1999, 475(Pt. 2, Appl. Accelerators Res. and Ind.), 854.
- 85 F. P. Santos, T. H. V. T. Dias, P. J. B. M. Rachinhas, C. A. N. Conde and A. D. Stauffer, IEEE Nucl. Sci. Symp. Conf.
- Rec. 1998, 1999, 1, 572.
 T. H. V. T. Dias, S. P. Santos, P. J. B. M. Rachinhas, F. I. G. M. Borges, J. M. F. dos Santos, C. A. N. Conde and
- A. D. Stauffer, *J. Appl. Phys.*, 1999, **85**(9), 6303. R. M. C. Silva and C. A. N. Conde, *IEEE Nucl. Sci. Symp. Conf.* Rec. 1998, 1999, 1, 714.
- J. F. Boyle, X-Ray Spectrom., 1999, 28(3), 178.
- X. G. Long, N. Huang, T. H. Li, F. Q. He and X. F. Peng, *Adv. X-Ray Anal.*, 1998, **40**, 307. 89
- 90 I. Facchin, C. Mello, M. I. M. S. Bueno and R. J. Poppi, X-Ray Spectrom., 1999, 28(3), 173.
- 91
- S. X. Bao, *X-Ray Spectrom.*, 1999, **28**(3), 141. P. Lemberge and P. Van Espen, *X-Ray Spectrom.*, 1999, **28**(2), 77. 92
- 93
- P. O. Verkhovodov, Adv. X-Ray Anal., 1998, 40, 315. V. A. Simakov and V. E. Isaev, J. Anal. Chem. (Transl. of Zh. 94 Anal. Khim.), 1999, 54(7), 612.
- 95 F. A. Weber, L. B. Da Silva, T. W. Barbee Jr., D. Ciarlo and M. Mantler, Adv. X-Ray Anal., 1998, 40, 298.
- H. Ebel, X-Ray Spectrom., 1999, 28, 255.
- N. Broll and P. de Chateaubourg, Adv. X-Ray Anal., 1999, 41,
- E. Acosta, X. Llovet, E. Coleoni, F. Salvat and J. A. Riveros, X-Ray Spectrom., 1999, 28(2), 121.
- G. R. Lachance, Adv. X-Ray Anal., 1999, **41**, 718. H. C. C. Cloete, Adv. X-Ray Anal., 1999, **41**, 743. K. K. Padhi, NML Tech. J., 1998, **40**(2), 63.
- 100
- 101
- G. V. Pavlinsky and L. I. Vladimirova, X-Ray Spectrom., 1999, 102 **28**(3), 183.
- 103
- M. Garcia and R. Figueroa, Adv. X-Ray Anal., 1999, 41, 788. L. Vincze, K. Janssens, B. Vekemans and F. Adams, X-Ray 104 Spectrom., 1999, 54B(12), 1711.
- D. U. Rashmi and D. K. Suri, X-Ray Spectrom., 1999, 28(3), 157. 105
- 106 S. X. Bao, Guangpuxue Yu Guangpu Fenxi, 1999, 19(1), 90.
- 107 S. Bao, Z. Wang and L. Rong, Guangpuxue Yu Guangpu Fenxi, 1999, 19(2), 221.
- 108 P. Duvauchelle, G. Peix and D. Babot, Nucl. Instrum. Methods Phys. Res., Sect. B, 1999, 155(3), 221.
- 109 A. Kuczumow, B. Vekemans, O. Schalm, L. Vincze, W. Dorrine,
- K. Gysels and R. Van Grieken, X-Ray Spectrom., 1999, 28, 282. R. Willingale, Lect. Notes Phys., 1999, 520(X-Ray Spectroscopy 110 in Astrophysics), 435.
- B. Adams, T. Hiort, E. Kossel, G. Materlik, Y. Nishino and D. V. Novikov, Phys. Status Solidi B, 1999, 215(1), 757.
- R. Hudec, P. Ladislav, I. Adolf and J. Thieme, Replicated X-ray optics. X-Ray Microsc. Spectromicrosc., Status Rep. Int. Conf., 5th [computer optical disk] 1996, Springer, Berlin, Germany, 1998, 265–269.
- 113 V. V. Aristov and J. Thieme, Bragg-Fresnel optics. X-Ray Microsc. Spectromicrosc., Status Rep. Int. Conf., 5th [computer optical disk] 1996, Springer, Berlin, Germany, 1998, 30-36.

- 114 Ch. Morawe, P. Pecci, J. Ch. Peffen and E. Ziegler, Rev. Sci. Instrum., 1999, 70(8), 3227.
- K. Tamura, K. Yamashita, H. Kunieda, T. Yoshioka, M. Watanabe and K. Haga, Proc. SPIE-Int. Soc. Opt. Eng., 1999, 3766(X-Ray Optics, Instruments, and Missions II), 371.
- I. V. Kozhevnikov, I. N. Bukreeva and E. Ziegler, Proc. SPIE-Int. Soc. Opt. Eng., 1998, 3448(Crystal and Multilayer Optics),
- 117 A. Bakulin, S. M. Durbin, C. Liu, J. Erdmann, A. T. Macrander and T. Jach, Proc. SPIE-Int. Soc. Opt. Eng., 1998, 3448(Crystal and Multilayer Optics), 218.
- Z. Wang, Y. Ma, J. Cao, X. Chen, X. Xu, Y. Hong and S. Fu, Proc. SPIE-Int. Soc. Opt. Eng., 1998, 3448(Crystal and Multilayer Optics), 332.
- H. Ohmori, S. Moriyasu, Y. Yamagata, A. Makinouchi, H. Asama, I. Takahashi, N. Itoh and T. Nakagawa Inst. Phys. Conf. Ser., 1999, 159(X-Ray Lasers 1998), 619.
- N. Itoh, H. Ohmori, T. Kasai, T. Karaki-Doy and K. Horio, Inst. Phys. Conf. Ser., 1999, 159(X-Ray Lasers 1998), 623.
- N. Vachirapatama, M. Macka, B. Paull, C. Muenker and P. R. Haddad, *J. Chromatogr.*, *A*, 1999, **850**(1–2), 257. M. Ohmae, M. Konaka, M. Mori, H. Ohmori, Y. Yamagata,
- S. Moriyasu, N. Itoh and A. Makinouchi, Inst. Phys. Conf. Ser., 1999, 159(X-Ray Lasers 1998), 631.
- D. Ohara, Proc. SPIE-Int. Soc. Opt. Eng., 1998, 3444(X-Ray and Ultra-violet Spectroscopy and Polarimetry II), 98.
- A. A. Bzhaumikhov, N. Langhoff, J. Schmalz, R. Wedell, V. I. Beloglazov and N. F. Lebedev, *Proc. SPIE-Int. Soc. Opt.* Eng., 1998, 3444(X-Ray Optics, Instruments and Missions), 430.
- S. V. Nikitina, A. S. Shcherbakov and N. S. Ibraimov, Rev. Sci. Instrum., 1999, 70(7), 2950.
- S. V. Nikitina, N. S. Ibraimov and A. S. Stcherbakov, Proc. SPIE-Int. Soc. Opt. Eng., 1998, 3444(X-Ray Optics, Instruments and Missions), 451.
- J. Gormley, T. Jach, E. Steel and Q. F. Xiao, X-Ray Spectrom., 1999, 28(2), 115.
- Y. L. Ding, J. J. He, F. Z. Wei, J. D. Xie, D. C. Wang, Y. Li, B. Z. Chen, J. Chen and Y. M. Yan, Adv. X-Ray Anal., 1999, 41, 243.
- V. A. Arkadiev, H.-E. Gorny, W. Scholz and R. Wedell, Use of 129 glass capillaries for microspot XRF analysis. X-Ray Microsc. Spectromicrosc., Status Rep. Int. Conf., 5th 1996, Springer, Berlin, Germany, 1998, 37-41.
- M. Haschke and U. Theis, GIT Labor-Fachz., 1999, 43(5), 458.
- J. A. Nicolosi, B. Scruggs and M. Haschke, Adv. X-Ray Anal., 1999, 41, 227.
- B. Kanngiesser, B. Beckhoff, W. Malzer, V. A. Arkadiev, A. A. Bzhaumikhov and H.-E. Gorny, Adv. X-Ray Anal., 1998, **40**, 191.
- D. Wegrzynek, B. Holynska and J. Ostachowicz, X-Ray Spectrom., 1999, 28, 209.
- D. Ohara, Proc. SPIE-Int. Soc. Opt. Eng., 1998, 3443(X-Ray and
- Ultraviolet Spectroscopy and Polarimetry II), 128. A. K. Cheburkin and W. Shotyk, *X-Ray Spectrom.*, 1999, **28**(5), 379.
- K. Schmetzer, Z. Beili, G. Yan, H.-J. Bernhardt and H. A. Hanni, J. Gemmol., 1999, 26(5), 289.
- 137 G. J. Havrilla and J. R. Schoonover, Mater. World, 1999, 7(10),
- P. Hammersberg, M. Stenstrom, H. Hedtjarn and M. Mangard, J. X-Ray Sci. Technol., 1998, 8(1) (Ed.), 5.
- D. C. Sigee, J. Morgan, A. T. Sumner and A. Warley, X-ray microanalysis in biology, Cambridge University Press, Cambridge, UK, 1993, 0 521 41530 6, 351 pp.
- P. Chevallier, P. Populus and A. Firsov, X-Ray Spectrom., 1999, **28**(5), 348.
- A. K. Freund, Synchrotron X-ray beam optics. Complementarity Neutron Synchrotron X-ray Scattering, Proc. Summer Sch. Neutron Scattering, 6th 1998, World Scientific, Singapore, 1998, 329–349.
- S. R. Sutton and M. L. Rivers, CMS Workshop Lect., 1999, 9(Synchrotron X-ray Methods in Clay Science), 146.
- F. Adams, Curr. Trends Anal. Chem., 1998, 1, 49.
- J. P. F. Sellschop, Proc. SPIE-Int. Soc. Opt. Eng., 1998, 3448(Crystal and Multilayer Optics), 40.
- A. K. Freund, J. P. F. Sellschop, K. Lieb, S. Rony, C. Schulze, L. Schroeder and J. Teyssier, Proc. SPIE-Int. Soc. Opt. Eng., 1998, 3448(Crystal and Multilayer Optics), 53.
- J. C. Lang, G. Srajer, J. Wang and P. L. Lee, Rev. Sci. Instrum., 146 1999, **70**(12), 4457.

- 147 O. Chubar and P. Elleaume, EPAC-98, Eur. Part. Accel. Conf., 6th, 1998, 1998, 2, 1177.
- M. Sanchex Del Rio and R. J. Dejus, Proc. SPIE-Int. Soc. Opt. 148 Eng., 1998, 3448(Crystal and Multilayer Optics), 340.
- 149 S. Hayakawa, A. Yamaguchi, W. Hong, Y. Gohshi, T. Yamamoto, K. Hayashi, J. Kawai and S. Goto, Spectrochim. Acta, Part B, 1999, 54, 171.
- Y. Terada, N. Kondo, M. Kataoka, M. Izumiyama, I. Nakai and S. Goto, X-Ray Spectrom., 1999, **28**(6), 461. K. Sakurai and H. Eba Jpn. J. Appl. Phys., Part 1, 1999,
- 38(Suppl. 1, Synchrotron Radiation in Materials Science), 650.
- C. A. Perez, M. Radtke, H. J. Sanchez, H. Tolentino, R. T. Neuenshwander, W. Barg, M. Rubio, M. I. Silveira 152 Bueno, I. M. Raimundo and J. J. R. Rohwedder, X-Ray Spectrom., 1999, 28(5), 320.
- M. Mosbah, J. P. Duraud, N. Metrich, Z. Wu, J. S. Delaney and A. San Miguel, Nucl. Instrum. Methods Phys. Res., Sect. B, 1999, **158**(1-4), 214.
- K. Takada, A. M. Ektessabi and S. Yoshida, AIP Conf. Proc. 1999, 475(Pt. 1, Application of Accelerators in Research and Industry), 452.
- 155 T. H. Hansteen, P. M. Sachs and F. Lechtenberg, Eur. J. Mineral., 2000, 12(1), 25.
- K. Janssens, L. Vincze, B. Vekemans, C. T. Williams, M. Radtke, 156 M. Haller and A. Knoechel, Fresenius' J. Anal. Chem., 1999, 363(4), 413.
- 157 W. Nozaki, T. Nakamura, A. Iida, K. Matsuoka and N. Takaoka, Antarct. Meteorite Res., 1999, 12, 199.
- 158 M. O. Figueiredo, M. T. Ramos, T. Pereira da Silva, M. J. Basto and P. Chevallier, X-Ray Spectrom., 1999, 28, 251.
- 159 A. Berglund, H. Brelid, A. Rindby and P. Engstrom, Holzforschung, 1999, 53(5), 474.
- R. R. Martin, T. K. Sham, G. W. Won, P. Van Der Heide, K. W. Jones, S.-R. Song and R. Protz, Can. J. For. Res., 1998, 28(10), 1464.
- M. A. Zaitz and P. Wobrauschek, Proceedings of the 7th 161 Conference on Total Reflection X-ray Fluorescence Analysis and Related Methods (TXRF'98), held 27 September–3 October 1998, in Austin, Texas. Spectrochim. Acta, Part B, 1999; 54B(10), Elsevier, Amsterdam, Netherlands, 1999, 161 pp.
- K. Sakurai, Spectrochim. Acta, Part B, 1999, 54(10), 1497.
- 163 J. Knoth, P. A. Beaven, C. Michaelsen, H. Schneider and H. Schwenke, X-Ray Spectrom., 1999, 28(2), 110.
- 164 R. Schwaiger, P. Wobrauschek and C. Streli, Adv. X-Ray Anal., 1999, 41, 804.
- K. Tsuji, T. Sato, K. Wagatsuma, M. Claes and R. Van Grieken, 165 Rev. Sci. Instrum., 1999, 70(3), 1621.
- R. Padilla Alvarez, E. Chinea Cano, J. R. Estevez Alvarez and 166 E. D. Greaves, J. Radioanal. Nucl. Chem., 1999, 240(2), 517.
- V. F. N. Filho, V. H. Poblete, P. S. Parreira, E. Matsumoto, S. M. Simabuco, E. P. Espinoza and A. A. Navarro, Biol. Trace Elem. Res., 1999, 71, 423.
- M. Theisen and R. Niessner, Spectrochim. Acta, Part B, 1999, 168 54B(13), 1839.
- A. Prange, U. Reus, H. Schwenke and J. Knoth, Spectrochim. 169 Acta, Part B, 1999, 54(10), 1505.
- 170 J. Knoth, A. Prange, U. Reus and H. Schwenke, Spectrochim. Acta, Part B, 1999, 54(10), 1513.
- 171 I. Szaloki, T. Utaka, Y. Tsuji and K. Taniguchi, Adv. X-Ray Anal., 1999, 41, 812.
- C. Streli, P. Kregsamer, P. Wobrauschek, H. Gatterbauer, P. Pianetta, S. Pahlke, L. Fabry, L. Palmetshofer and 172 M. Schmeling, Spectrochim. Acta, Part B, 1999, 54B(10), 1433.
- K. Sakurai, H. Eba and S. Goto, Jpn. J. Appl. Phys., Part 1, 1999, 38(Suppl. 1, Synchrotron Radiation in Materials Science), 332.
- F. Comin, M. Navizet, P. Mangiagalli and G. Apostolo, Nucl. Instrum. Methods Phys. Res., Sect. B, 1999, **B150**(1-4), 538.
- F. Comin, Proc. Electrochem. Soc., 1999, 99(Analytical and 175 Diagnostic Techniques for Semiconductor Materials, Devices and Processes), 134.
- 176 F. Comin, G. Apostolo, A. Freund, P. Mangiagalli, M. Navizet and C. L. Troxel, Proc. SPIE-Int. Soc. Opt. Eng., 1998, 3448(Crystal and Multilayer Optics), 11.
- 177 H. Kim and K. Ryoo, Han'guk Pyomyon Konghak Hoechi, 1999,
- H. Gatterbauer, P. Wobrauschek, F. Hegedus, P. Boni and C. Streli, Adv. X-Ray Anal., 1999, 41, 379.
- N. S. Shin, Y. M. Koo, C. H. Chang and H. Padmore, J. Appl. Phys., 1999, 86(2), 902.
- 180 P. Kregsamer, C. Streli, P. Wobrauschek, H. Gatterbauer,

- P. Pianetta, L. Palmetshofer and L. L. Brehm, X-Ray Spectrom., 1999, 28, 292.
- A. Huber and F. Freudenberg, Proc. Electrochem. Soc., 1999, 16(Analytical and Diagnostic Techniques for Semiconductor Materials, Devices and Processes), 221.
- 182 M. Funahashi, M. Matsuo, N. Kawada, M. Yamagami and R. Wilson, Spectrochim. Acta, Part B, 1999, 54(10), 1409.
- M. Yamagami, M. Nonoguchi, T. Yamada, T. Shoji, T. Utaka, Y. Mori, S. Nomura, K. Taniguchi, H. Wakita and S. Ikeda, Bunseki Kagaku, 1999, 48(11), 1005.
- G. Buhrer, Spectrochim. Acta, Part B, 1999, 54(10), 1399
- M. Yamagami, M. Nonoguchi, T. Yamada, T. Shoji, T. Utaka, S. Nomura, K. Taniguchi, H. Wakita and S. Ikeda, X-Ray Spectrom., 1999, 28(6), 451.
- L. Fabry, S. Pahlke, L. Kotz, P. Wobrauschek and C. Streli, Fresenius' J. Anal. Chem., 1999, 363(1), 98.
 G. Vereecke, M. Schaekers, K. Verstraete, S. Arnauts,
- M. M. Heyns and W. Plante, *Proc. Electrochem. Soc.*, 1999, 16(Analytical and Diagnostic Techniques for Semiconductor Materials, Devices and Processes), 139.
- R. Klockenkaemper and A. von Bohlen, Spectrochim. Acta, Part B, 1999, **54**(10), 1385.
- R. Klockenkaemper, A. von Bohlen, H. W. Becker and L. Palmetshofer, Surf. Interface Anal., 1999, 27(11), 1003.
- I. Rink and H. Thewissen, Spectrochim. Acta, Part B, 1999, **54**(10), 1427.
- K. Iltgen, E. Zschech, A. Ghatak-Roy and T. Hossain, Spectrochim. Acta, Part B, 1999, 54(10), 1393.
- K. Iltgen, B. MacDonald, O. Brox, A. Benninghoven, C. Weiss, T. Hossain and E. Zschech, AIP Conf. Proc., 1998, 449(Characterization and Metrology for ULSI Technology), 777.
- Y. Mori and K. Uemura, X-Ray Spectrom., 1999, 28(6), 421
- B. W. Liou and C. L. Lee, Chin. J. Phys. (Taipei), 1999, 37(6),
- D. Werho, R. B. Gregory, S. N. Schauer, X. Liu, G. F. Carney, J. C. Banks, J. A. Knapp, B. L. Doyle and A. C. Diebold, Adv. X-Ray Anal., 1998, 40, 37.

 D. Werho, T. Wetteroth, S. N. Schauer and G. F. Carney, Adv.
- X-Ray Anal., 1998, 40, 48.
- Z. M. Spolnik, M. Claes and R. van Grieken, Anal. Chim. Acta, 1999, **401**(1–2), 293. M. Claes, R. Van Ham, K. Janssens, R. Van Grieken,
- 198 R. Klockenkamper and A. von Bohlen, Adv. X-Ray Anal., 1999, 41, 262.
- M. Schmeling and R. Van Grieken, Determination of light elements in marine aerosols by grazing-emission X-ray fluorescence. Proc. EUROTRAC Symp. '98: Transp. Chem. Transform. Troposphere 1998, WIT Press, Southampton, UK, 1999, 340-343.
- M. Claes, K. van Dyck, H. Deelstra and R. van Grieken, Spectrochim. Acta, Part B, 1999, 54(10), 1517.
- M. Claes, P. de Bokx and R. Van Grieken, X-Ray Spectrom., 1999, 28, 224.
- K. Tsuji, H. Takenaka, K. Wagatsuma, P. K. de Bokx and R. E. Van Grieken, Spectrochim. Acta, Part B, 1999, 54B(13), 1881
- Z. M. Spolnik, M. Claes, R. E. van Grieken, P. K. de Bokx and
- H. P. Urbach, Spectrochim. Acta, Part B, 1999, 54(10), 1525. A. Kuczumow, M. Claes, M. Schmeling, R. Van Grieken and S. de Gendt, J. Anal. At. Spectrom., 2000, 15(4), 415.
- C. Kok and H. P. Urbach, On the regularization of the inverse Laplace transform in grazing-emission X-ray fluorescence spectroscopy. Inverse Probl. Eng., Gordon & Breach Science Publishers, 1999, 433–470.
- K. Tsuji, Z. Spolnik, K. Wagatsuma, J. Zhang and R. E. Van Grieken, Spectrochim. Acta, Part B, 1999, 54, 1243.
- 207 K. Tsuji, R. Nullens, K. Wagatsuma and R. E. Van Grieken, J. Anal. At. Spectrom., 1999, 14(11), 1711.
- A. Ritschel, P. Wobrauschek, E. Chinea, F. Grass and C. Fabjan, Spectrochim. Acta, Part B, 1999, 54(10), 1449.
- L. Bennun, V. H. Gillette and E. D. Greaves, Spectrochim. Acta, Part B, 1999, 54, 1291.
- M. Theisen and R. Niessner, Fresenius' J. Anal. Chem., 1999, **365**(4), 332.
- J. Dixkens and H. Fissan, Aerosol Sci. Technol., 1999 (5), 438.
- J. K. Vilhunen, A. von Bohlen, M. Schmeling, L. Rantanen, S. Mikkonen, R. Klockenkaemper and D. Klockow, Mikrochim. Acta, 1999, 131(3-4), 219.
- N. Kallithrakas-Kontos and G. Kavelaki, (Dept. Sci., Lab. Anal. Environ. Chem., Tech. Univ. Crete, 73100 Chania, Greece). Presented at Instrumental Methods of Analysis. Modern Trends

- and Applications (IMA '99), 19-22 September, 1999, Chalkidiki, Greece
- E. H. Bakraji and J. Karajo, Water Qual. Res. J. Can., 1999, 214 34(2), 305.
- 215 T. Capote, L. M. Marco, J. Alvarado and E. D. Greaves, Spectrochim. Acta, Part B, 1999, 54(10), 1463.
- A. Viksna, V. Znotina and J. Boman, X-Ray Spectrom., 1999, 28, 216
- M. Olsson, A. Viksna and H.-S. Helmisaari, X-Ray Spectrom., 217 1999, 28(5), 335.
- B. Holynska, B. Ostachowicz and L. Samek, X-Ray Spectrom., 1999, 28(5), 372.
- 219 M. M. Costa, M. A. Barreiros, M. L. Carvalho and I. Queralt, X-Ray Spectrom., 1999, 28(5), 410.

 I. Queralt, M. A. Barreiros, M. L. Carvalho and M. M. Costa,
- 220 Sci. Total Environ., 1999, 241(1-3), 39.
- A. Varga, R. M. Garcinuno Martinez, G. Zaray and F. Fodor, 221 Spectrochim. Acta, Part B, 1999, **54**(10), 1455. E. Tatar, V. G. Mihucz, A. Varga, G. Zaray and E. Cseh, J. Inorg.
- 222
- Biochem., 1999, 75(3), 219. L. M. Marco, E. D. Greaves and J. Alvarado, Spectrochim. Acta, 223 Part B, 1999, **54**(10), 1469.
- A. Kubala-Kukus, J. Braziewicz, D. Banas, U. Majewska, S. Gozdz and A. Urbaniak, Nucl. Instrum. Methods Phys. Res., Sect. B, 1999, B150(1-4), 193.
- R. F. Ruiz, J. D. Tornero, V. M. Gonzalez and C. Alonso, Analyst (Cambridge, U. K.), 1999, 124(4), 583. 225
- 226 G. Bellisola, F. Pasti, M. Valdes and A. Torboli, Spectrochim. Acta, Part B, 1999, 54(10), 1481.
- 227 U. Majewska, J. Braziewicz, D. Banas, A. Kubala-Kukus, S. Gozdz, M. Pajek, M. Zadrozna, M. Jaskola and T. Czyzewski, Nucl. Instrum. Methods Phys. Res., Sect. B, 1999, 150(1-4), 254.
- A. Kelko-Levai, I. Varga, K. Zih-Perenyi and A. Lasztity, Spectrochim. Acta, Part B, 1999, 54, 827. 228
- R. Klockenkaemper, A. von Bohlen and L. Moens, X-Ray Spectrom., 2000, 29, 119.
- A. von Bohlen, J. Trace Microprobe Tech., 1999, 17(2), 177.
- C. Fiorini, A. Longoni, M. Milazzo and F. Zaraga, IEEE Nucl. 231
- Sci. Symp. Conf. Rec. 1998, 1999, 1, 375.

 A. K. Khusainov, T. A. Antonova, S. V. Bahlanov, A. V. Derbin, V. V. Ivanov, V. V. Lysenko, F. Morozov, V. G. Mouratov, V. N. Muratova, Y. A. Petukhov, A. M. Pirogov, O. P. Polytsia, V. D. Saveliev, V. A. Solovei, K. A. Yegorov and M. P. Zhucov, Nucl. Instrum. Methods Phys. Res., Sect. A, 1999, 428(1), 223.
- M. D. Goldthorp, P. Lambert and M. Fingas, Person-portable analytical systems project. Proc.-Tech. Semin. Chem. Spills, 14th 1997, Environment Canada, Ottawa, Ontario, Canada, 1997, 75-
- 234 J. Flachowsky, A. Rammler, Th. Arthen-Engeland and J. Stach, AT-PROCESS, 1999, 4(3-4), 52.
- V. V. Moreplavtsev and V. I. Tarakanovskii, Razved. Okhr. Nedr, 235 1998 (12), 23.
- M. Ridings, A. J. Shorter, J. Bawden-Smith and C. D. Johnston, Strategies for the investigation of contaminated sites using field portable X-ray fluorescence (FPXRF) techniques. Contam. Site Rem.: Challenges Posted Urban Ind. Contam., Proc. Contam. Site Rem. Conf., Centre for Groundwater Studies, Wembley, Australia, 1999, 213–217.
- 237 J. F. Schneider, D. Johnson, N. Stoll and K. Thurow, AT-PROCESS, 1999, 4(1-2), 12.
- R. J. VanCott, B. J. McDonald and A. G. Seelos, Nucl. Instrum. 238 Methods Phys. Res., Sect. A, 1999, 422(1-3), 801. P. Anderson, C. M. Davidson, D. Littlejohn, A. M. Ure,
- 239 L. M. Garden and J. Marshall, Int. J. Environ. Anal. Chem., 1998, 71(1), 19.
- 240 B. J. McDonald, C. W. Unsell, W. T. Elam, K. R. Hudson and J. W. Adams, Nucl. Instrum. Methods Phys. Res., Sect. A, 1999, **422**(1-3), 805.
- S. Clark, W. Menrath, M. Chen, S. Roda and P. Succop, Ann. Agric. Environ. Med., 1999, 6(1), 27.
- S. Clark, W. Menrath, M. Chen, S. Roda and P. Succop, Use of a field portable X-ray fluorescence analyzer to determine the concentration of lead and other metals in soil and dust samples. Warsaw '98, Int. Symp. Exhib. Environ. Contam. Cent. East. Eur., Symp. Proc., 4th, Florida State University, Tallahassee, FL, USA, 1998, 1313-1319.
- 243 J. C. Morley, C. S. Clark, J. A. Deddens, K. Ashley and S. Roda, Appl. Occup. Environ. Hyg., 1999, 14(5), 306.
- R. L. Schmehl, D. C. Cox, F. G. Dewalt, M. M. Haugen, R. A. Koyak, J. G. Schwemberger Jr. and J. V. Scalera, Am. Ind. Hyg. Assoc. J., 1999, 60(4), 444.

- 245 R. Cesareo, A. Castellano, G. Buccolieri and M. Marabelli, Nucl. Instrum. Methods Phys. Res., Sect. B, 1999, B155(3), 326.
- G. Vittiglio, K. Janssens, B. Vekemans, F. Adams and A. Oost, Spectrochim. Acta, Part B, 1999, 54B(12), 1697.
- P. Moioli and C. Seccaroni, X-Ray Spectrom., 2000, 29, 48.
- G. W. Fraser, Lect. Notes Phys., 1999, 520(X-Ray Spectroscopy 248 in Astrophysics), 477.
- F. Paerels, Lect. Notes Phys., 1999, 520(X-Ray Spectroscopy in Astrophysics), 347.
- H. Y. McSween Jr., S. L. Murchie, J. A. Crisp, N. T. Bridges, R. C. Anderson, J. F. Bell III, D. T. Britt, J. Bruckner, G. Dreibus, T. Economou, A. Ghosh, M. P. Golombek, J. P. Greenwood, J. R. Johnson, H. J. Moore, R. V. Morris, T. J. Parker, R. Rieder, R. Singer and H. Wanke, J. Geophys. Res., [Planets], 1999, 104(E4), 8679.
- H. E. Newsom, J. J. Hagerty and F. Goff, J. Geophys. Res., [Planets], 1999, 104(E4), 8717.
 V. M. Radchenko, B. M. Andreichikov, H. Wanke, B. D. Gaveilov, B. N. Korchuganov, R. Rieder, M. A. Ryabinin and T. Economou, Radiochemistry, 1999, 41(2), 155.
- T. Okada, M. Kato, A. Fujimura, H. Tsunemi and S. Kitamoto, Adv. Space Res., 1999, 23(11), 1833.
- Y. Kamata, T. Takeshima, T. Okada and K. Terada, Adv. Space Res., 1999, 23(11), 1829.
- 255 I. Nelson, U.S. US 5,982,847 (Cl. 378-47; G01N23/223), 9 Nov 1999, US Appl. 29,490, 28 Oct 1996; 21 pp.
- R. C. Tisdale, Tech. Pap. ISA, 1999, 393(Solutions for Improving Productivity and Flexibility), 45.
- R. C. Tisdale, AT-PROCESS, 1999, 4(1-2), 18.
- C. Bachmann and T. Sauer, Schuettgut, 1999, 5(3), 362.
- 259 S. T. Pedersen and M. S. Finney, Cem.-Hormigon, 1999, 70(801),
- A. H. Nahle, F. C. Walsh, C. Brennan and K. J. Roberts, J. Appl. 260 Crystallogr., 1999, 32(2), 369
- R. Harmel, O. Haupt and W. Dannecker, Fresenius' J. Anal. 261 Chem., 2000, 366(2), 178.
- O. Haupt, R. Harmel and W. Dannecker, *Adv. X-Ray Anal.*, 1999, **41**, 760. 262
- L. P. Colletti and G. J. Havrilla, Adv. X-Ray Anal., 1999, 41, 291. 263
- 264 K. Sugihara, K. Tamura, M. Sato and K. Ohno, X-Ray Spectrom., 1999, 28(6), 446.
- 265 A. W. Wilson, D. C. Turner and A. A. Robbins, Adv. X-Ray Anal., 1999, 41, 301.
- 266 H. Yamaguchi, S. Itoh, S. Igarashi, K. Naitoh and R. Hasegawa, Bunseki Kagaku, 1999, **48**(9), 855.
- J. J. Wachal and R. J. Riester, Proc. Int. Conf. Cem. Microsc., 1999, 21st, 1.
- S. Kurunczi, S. Torok and J. W. Beal, X-Ray Spectrom., 1999, **28**(5), 352.
- M. E. McComb and H. D. Gesser, Talanta, 1999, 49, 869.
- I. E. De Vito, A. N. Masi and R. A. Olsina, Talanta, 1999, 49, 270
- Y. N. Makarovskaya, L. P. Eksperiandova and A. B. Blank, J. Anal. Chem. (Transl. of Zh. Anal. Khim.), 1999, 54(11), 1031.
- K. N. Belikov, A. B. Blank, N. I. Shevtsov, O. Yu. Nadzhafova and M. M. Tananaiko, Anal. Chim. Acta, 1999, 383(3), 277.
- M. El Maghraoui, J.-L. Joron, J. Etoubleau, P. Cambon and M. Treuil, Geostand. Newsl., 1999, 23(1), 59.
- J. Etoubleau, P. Cambon, H. Bougault and J.-L. Joron, Geostand. Newsl., 1999, 23(2), 187.
- A. N. Masi and R. A. Olsina, J. Trace Microprobe Tech., 1999, 275 **17**(3), 315.
- B. D. Wheeler, Rigaku J., 1999, 16(1), 16.
- D. M. Johnson, P. R. Hooper and R. M. Conrey, Adv. X-Ray Anal., 1999, 41, 843.
- V. Y. Borkhodoev, J. Anal. Chem. (Transl. of Zh. Anal. Khim.), 1999, 54(5), 396.
- T. S. Aisueva and T. N. Gunicheva, J. Anal. Chem. (Transl. of Zh. Anal. Khim.), 1999, **54**(11), 1085.
- I. Szaloki, A. Somogyi, M. Braun and A. Toth, X-Ray Spectrom., 1999, **28**(5), 399.
- I. J. Funtua, J. Trace Microprobe Tech., 1999, 17(3), 293.
- M. E. Lipschultz, S.F. Wolf, J. M Hanchar and F.B. Culp, Anal. Chem., 1999, 71, 1R.
- J. G. Watson, J. C. Chow and C. A. Frazier, Adv. Environ., Ind. Process Control Technol., 1999, 1(Elemental Analysis of Airborne Particles), 67.
- K. Matsuda, S. Nakae and K. Miura, Taiki Kankyo Gakkaishi, 1999, **34**(3), 251.
- M. Fang, M. Zheng, F. Wang, K. S. Chim and S. C. Kot, Atmos. Environ., 1999, 33(11), 1803.

- G. Steinhoff, O. Haupt and W. Dannecker, Fresenius' J. Anal. 286 Chem., 2000, 366(2), 174.
- 287 C.-F. Wang, F.-H. Tu, S.-L. Jeng and C.-J. Chin, Gaodeng Xuexiao Huaxue Xuebao, 1999, 20(5), 70.
- 288 S. M. Talebi, Int. J. Environ. Anal. Chem., 1998, 72(1), 1.
- 289 H. K. Bandhu, S. Puri, M. L. Garg, B. Singh, J. S. Shahi, D. Mehta, E. Swietlicki, D. K. Dhawan, P. C. Mangal and N. Singh, Nucl. Instrum. Methods Phys. Res., Sect. B, 2000, **160**(1), 126.
- A. Chabas and R. A. Lefevre, Atmos. Environ., 1999, 34(2), 225.
- M. C. S. Seneviratne, P. Mahawatte, R. K. S. Fernando, R. Hewamanna and C. Sumithrarachchi, Biol. Trace Elem. Res., 1999, **71**, 189.
- 292 S. H. Cadle, P. A. Mulawa, E. C. Hunsanger, K. Nelson, R. A. Ragazzi, R. Barrett, G. L. Gallagher, D. R. Lawson, K. T. Knapp and R. Snow, Environ. Sci. Technol., 1999, 33(14), 2328.
- J. Zamurs, J. Bass, B. Williams, R. Fritsch, D. Sackett and 293 R. Heman, *Transp. Res. Rec.*, 1998, (1641), 29.

 A. Mendoza, R. Cesareo, M. Valdes, J. J. Meitin, R. Perez and V. Lorento, L. Padis and N. L. College, 1998, (1662), 1998, (1642), 1998
- 294 Y. Lorente, J. Radioanal. Nucl. Chem., 1999, 240(2), 459.
- 295 I. Orlic and S. M. Tang, Nucl. Instrum. Methods Phys. Res., Sect. *B*, 1999, **150**(1–4), 291.
- 296 T. Pinheiro, M. F. Araujo, P. M. Carreira, P. Valerio, D. Nunes and L. C. Alves, Nucl. Instrum. Methods Phys. Res., Sect. B, 1999, **150**(1-4), 306.
- 297 R. Wehausen, B. Schnetger, H.-J. Brumsack and G. J. De Lange, X-Ray Spectrom., 1999, 28(3), 168.
- A. T. Ellis, P. A. Russell and R. James, Adv. X-Ray Anal., 1998, 298 40, 329.
- 299 J. R. Schoonover and G. J. Havrilla, Appl. Spectrosc., 1999, 53(3), 257.
- 300 A. Janssen, P. Reichel and B. Wieschhorster, Labor Praxis, 1999, 23(7-8), 24.
- 301 W. Beckers, D. Schuller and O. Vaizert, J. Anal. Appl. Pyrolysis, 1999, **50**(1), 17.
- 302 J. Kierzek, B. Malozewska-Bucko, P. Bukowski, J. L. Parus, A. Ciurapinski, S. Zaras, B. Kunach and K. Wiland, J. Radioanal. Nucl. Chem., 1999, 240(1), 39.
- V. Sprta, B. Knob and P. Janos, Fresenius' J. Anal. Chem., 1999, 303 **364**(8), 705.
- Y. Zhang, J. L. Talbott, L. Wiedenmann, J. DeBarr and I. Demir, 304 Adv. X-Ray Anal., 1999, 41, 879.
- 305 A. I. Karayigit, D. A. Spears and C. A. Booth, Int. J. Coal Geol., 2000, 42(4), 297.
- 306 Z. Tekin and M. Tan, Spectrosc. Lett., 1999, 32(4), 661
- B. D. Kalinin, N. I. Karamyshev, R. I. Plotnikov, G. A. Pshenichnyi, M. V. Shimaraev, A. M. Nabokov, 307 N. M. Sorokina and G. I. Tsizin, Zavod. Lab., Diagn. Mater., 1998, 64(8), 15.
- 308 H. Kempter and B. Frenzel, Sci. Total Environ., 1999, 241(1-3),
- R. H. Lambert, K. Beach, J. Owens, J. Cooper, B. Johnsen and B. Richards, A continuous sampling system for hazardous element compliance assurance. Proc. Int. Conf. Incineration Therm. Treat. Technol., University of California, Irvine, CA, USA, 1998, 95-99.
- R. K. Dhir, P. C. Hewlett and T. D. Dyer, Cem. Concr. Res., 310 1999, 29(5), 667.
- J. A. Cooper, B. E. Johnsen, R. H. Lambert, K. Beach and 311 J. Owens, Second generation continuous sampling system for hazardous element compliance assurance based on XRF analysis. Proc. Int. Conf. Incineration Therm. Treat. Technol., Univ. California, Irvine, CA, USA, 1999, 547–551.
- N. A. H. Janssen, G. Hoek, B. Brunekreef and H. Harssema, Occup. Environ. Med., 1999, 56(7), 482.
- 313 M. R. Cave, O. Butler, J. M. Cook, M. S Cresser, L. M. Garden and D. L. Miles, J. Anal. At. Spectrom., 2000, 15(2), 181.
- M. Hall, C. Amraatuvshin and E. Erdenbat, J. Radioanal. Nucl. Chem., 1999, 240(3), 763.
- C. Punyadeera, A. E. Pillay, L. Jacobson and G. Whitelaw, J. Trace Microprobe Tech., 1999, 17(1), 63.
- 316 D. Adan-Bayewitz, F. Asaro and R. D. Giauque, Archaeometry, 1999, **41**(1), 1.
- A. E. Pillay, C. Punyadeera, L. Jacobson and J. Eriksen, *X-Ray Spectrom.*, 2000, **29**, 53. 317
- K. N. Yu and J. M. Miao, Appl. Radiat. Isot., 1999, 51(3), 279. 318
- 319 P. L. Leung and H. Luo, X-Ray Spectrom., 2000, 29, 34.
- G. Demortier, Y. Morciaux and D. Dozot, Nucl. Instrum. 320 Methods Phys. Res., Sect. B, 1999, B150(1-4), 640.
- 321 Z. W. Mao, Guangpuxue Yu Guangpu Fenxi, 1999, 19(5), 738.

- M. M. Al-Kofahi and K. F. Al-Tarawneh, X-Ray Spectrom., 322 2000, 29, 39,
- R. Klockenkamper, H. Bubert and K. Hasler, Archaeometry, 1999, 41(2), 311.
- M. Mantler and M. Schreiner, X-Ray Spectrom., 2000, 29, 3.
- 325 E. Aloupi, A. G. Karydas and T. Paradellis, X-Ray Spectrom., 2000, 29, 18.
- P. Leutenegger, A. Longoni, C. Fiorini, L. Struder, J. Kemmer, P. Lechner, S. Sciuti and R. Cesareo, Nucl. Instrum. Methods Phys. Res., Sect. A, 2000, 439(2-3), 458.
- J. L. Ferrero, C. Roldan, E. Navarro, M. Ardid, M. Marzal, J. Almirante, P. Ineba, J. Vergara and C. Mata, J. Radioanal. Nucl. Chem., 1999, 240(2), 523.
- J. L. Ferrero, C. Roldan, M. Ardid and E. Navarro, Nucl. Instrum. Methods Phys. Res., Sect. A, 1999, 422(1-3), 868.
- C. Neelmeijer, I. Brissaud, T. Calligaro, G. Demortier, A. Hautojarvi, M. Mader, L. Martinot, M. Schreiner, T. Tuurnala and G. Weber, X-Ray Spectrom., 2000, 29, 101.
- E. Panczyk, M. Ligeza and L. Walis, Czech. J. Phys., 1999, 49 330 (Suppl. 1, Pt. 1, 13th Radiochemical Conference, 1998), 401.
- P. Hoffmann, S. Bichlmeier, M. Heck, C. Theune and J. Callmer, X-Ray Spectrom., 2000, **29**, 92.
- P. Wobrauschek, G. Halmetschlager, S. Zamini, C. Jokubonis, G. Trnka and M. Karwowski, X-Ray Spectrom., 2000, 29, 25.
- Z. Smit, P. Pelicon, G. Vidmar, B. Zorko, M. Budnar, G. Demortier, B. Gratuze, S. Sturm, M. Necemer, P. Kump and M. Kos, Nucl. Instrum. Methods Phys. Res., Sect. B, 2000, 161, 718.
- F. Guo, X. J. Li and Z. Y. Chen, Guangpuxue Yu Guangpu Fenxi, 1999, **19**(3), 437. K. Cai, C. H. Li, Z. D. Liu and G. Y. Li, *Guangpuxue Yu*
- Guangpu Fenxi, 1999, 19(3), 441.
- G. Z. Hao, S. B. Bu, X. H. Gao and R. H. Xie, Fenxi Shiyanshi, 1999, **18**(6), 59.
- B. D. Kalinin and R. I. Plotnikov, Zavod. Lab., Diagn. Mater., 1998, 64(9), 29.
- E. Denes, P. J. Szabo and D. Zsambok, X-Ray Spectrom., 1999, 338 **28**, 267.
- J. L. Dobson, W. B. Cooley and J. E. Borst, Benefits of new generation laboratory automation. Electr. Furn. Conf. Proc., 1998, Iron and Steel Society, 1998, 783-788.
- W. Stankiewicz, B. Bolibrzuch and M. Marczak, Gold Bull. (London), 1998, 31(4), 119.
- A. M. Savolainen, D. J. Kinneberg, B. E. Mangion and L. J. Cabri, Preliminary analysis and method optimization based on X-ray fluorescence - application to precious metals. Anal. Technol. Miner. Ind., Proc. TMS Symp., TMS Annu. Meet., Minerals, Metals and Materials Soc., Warrendale, PA, USA, 1999, 55-71.
- 342 X. L. Wang, F. H. Cui, M. J. Li and F. X. Feng, Fenxi Shiyanshi, 1999, 18(1), 96.
- J. Fan, C. Q. Luo, W. Y. Huang, H. C. Yu, Z. Z. Zhang, H. Zou, D. L. Xiang, X. J. Mao, J. Wen and J. L. Yan, Lihua Jianyan, Huaxue Fence, 1999, 35(10), 451.
- D. Joseph and I. G. Sharma, J. Radioanal. Nucl. Chem., 1999,
- 240(1), 353.
 Z. T. Wang, S. Q. Niu and H. Deng, Guangpuxue Yu Guangpu
- Fenxi, 1999, **19**(1), 93. Y. Zhao and Z. T. Wang, Fenxi Shiyanshi, 1999, **18**(1), 19. 346
- C. M. Xu and B. J. Liu, Lihua Jianyan, Huaxue Fence, 1999, 347 **35**(2), 61.
- 348 J. P. Willis and E. B. McNew, Adv. X-Ray Anal., 1999, 41, 829.
- 349 G. Budak, A. Karabulut, O. Dogan and M. Levent, J. Trace Microprobe Tech., 1999, 17(3), 309.
- 350 G. Budak and A. Karabulut, Spectrochim. Acta, Part B, 1999, 54, 985.
- 351 I. I. Funtua, J. Trace Microprobe Tech., 1999, 17(2), 189.
- S. Wongnawa, P. Boonsin, D. Kongkaew, S. Yodbutra and S. Pisuttanawat, J. Trace Microprobe Tech., 1999, 17(1), 25.
- S. J. Zhuo, G. Y. Tao, Z. W. Yin and A. Ji, Lihua Jianyan, Huaxue Fence, 1999, 35(10), 435.
- H. Asakura, K. Ikegami and H. Wakita, Bunseki Kagaku, 1999, **48**(11), 973.
- A. Ji, S. J. Zhuo and G. Y. Tao, Lihua Jianyan, Huaxue Fence, 1999, 35(11), 483.
- A. Kern and S. Uhlig, Int. Cem. J., 1998, (2), 83.
- Anon. Int. Cem. J., 1998(2), 78. 357
- Ju. Iordanov, L. Vuchkova and A. Mitev, Anal. Lab., 1998, 7(4), 358
- M. Bettinelli, P. Fornasari, F. Bilei and M. Pesoli, Riv. Combust., 1998, **52**(5), 238.

- 360 S. Pessayre, R. Bacaud, C. Geantet and M. Vrina, Fuel, 1999, **78**(7), 857.
- 361 W. Njue, A. M. Kinyua and M. T. Thinguri, Bull. Chem. Soc. Ethiop., 1999, 13(2), 99.
- 362 M. Van Driessche and J. R. Sieber, Adv. X-Ray Anal., 1999, 41,
- H. Toersen and P. A. A. Slob, TriboTest, 1999, 5(3), 287. 363
- G. R. Humphrey, *Lubr. Eng.*, 1999, **55**(10), 19. R. R. Whitlock, *Adv. X-Ray Anal.*, 1998, **40**, 243. 364
- R. R. Whitlock, G. R. Humphrey and D. B. Churchill, Lubr. Eng., 1999, 55(10), 27
- R. W. Ryon and W. D. Ruhter, X-Ray Spectrom., 1999, 28, 230.
- P. J. A. Howarth, G. Uchiyama, T. Asakura, M. Sawada, H. Hagiya and S. Fujine, *JAERI-Conf.*, 1999, 99(Pt. 2, Proceedings of the NUCEF International Symposium, 1998),
- P. J. A. Howarth, G. Uchiyama, T. Asakura, M. Sawada, 369 H. Hagiya, S. Usuda and S. Fujine, Nucl. Mater. Manage., 1998, **27**(2), 977.
- J. L. Parus, W. Raab and R. Mikolajczak, Adv. X-Ray Anal., 370 1998, 40, 339,
- W. E. Swartz, Nucl. Mater. Manage., 1998, 27(2), 970.
- C. Cuhls, C. Schoneborn, M. Kraus, F. Jaekel and E. Schnoor, 372 Muell Abfall, 1999, 31(12), 716.
- I. Amano and S. Nishikata, Jpn. Kokai Tokkyo Koho JP 2000 28,565 (Cl. G01N27/22), 28 Jan 2000, Appl. 1998/196,876, 13 Jul 1998; 5 pp.
- G. Van Dalen, X-Ray Spectrom., 1999, 28(3), 149. 374
- P. Thebock, P. Hils and D. Damjanovic, Eur. Pat. Appl. EP 375 911,626 (Cl. G01N23/223), 28 Apr 1999, GB Appl. 97/22,475, 25 Oct 1997; 12 pp.
- F. E. McNeill and J. M. O'Meara, Adv. X-Ray Anal., 1999, 41,
- B.-K. Lee, Toxicol. Lett., 1999, 108(2-3), 149.
- 378 D. A. Bradley and M. J. Farquharson, X-Ray Spectrom., 1999, **28**. 270.
- 379 M. J. Farquharson and D. A. Bradley, Phys. Med. Biol., 1999, 44(4), 955.
- 380 D. A. Bradley, L. Kissel and R. H. Pratt, X-Ray Spectrom., 1999, **28**(5), 339.
- I. Szaloki, D. G. Lewis, C. A. Bennett and A. Kilic, Phys. Med. 381 Biol., 1999, 44(5), 1245.
- R. Speller, X-Ray Spectrom., 1999, 28, 244. 382
- 383 A. Aro, C. Amarasiriwardena, M.-L. Lee, R. Kim and H. Hu, Med. Phys., 2000, 27(1), 119.
- 384 Q. Ao, S. H. Lee and R. P. Gardner, Adv. X-Ray Anal., 1999, 41, 898.
- 385 Q. Ao, S. H. Lee and R. P. Gardner, Adv. X-Ray Anal., 1999, 41,
- L. Gerhardsson, J. Borjesson, S. Mattsson, A. Schutz and 386 S. Skerfving, Environ. Res., 1999, 80(4), 389.
- V. Potula, J. Serrano, D. Sparrow and H. Hu, J. Occup. Environ. 387 Med., 1999, 41(5), 349.
- 388 J. F. Rosen, Adv. Mod. Environ. Toxicol., 1998, 25(Hazardous Waste: Toxicology and Health Effects), 137.
- 389 D. E. B. Fleming, D. R. Chettle, C. E. Webber and E. J. O'Flaherty, Toxicol. Appl. Pharmacol., 1999, 161(1), 100.
- V. Zaichick, N. Ovchjarenko and S. Zaichick, Appl. Radiat. Isot., 390 1999, **50**(2), 283.
- P. L. Leung, H. M. Huang, D. Z. Sun and M. G. Zhu, Biol. Trace 391
- Elem. Res., 1999, **69**(3), 269. V. Y. Zaichick and S. V. Zaichick, J. Trace Microprobe Tech., 392 1999, **17**(2), 219.
- Y. Muramatsu, Y. Ishikawa, S. Yoshida and T. Mori, Radiat. 393 Res., 1999, 152(6, Suppl.), S97.
- 394 E. Halmagean, D. Loukas, M. Iacob and A. G. Karydas, X-Ray Spectrom., 1999, 28(5), 317.
- 395 B. Forslind, Nucl. Instrum. Methods Phys. Res., Sect. B, 1999, **150**(1-4), 150.
- A. Taylor, S. Branch, D. J. Halls, L. M. W. Owen and M. White, 396 J. Anal. At. Spectrom., 2000, 15(4), 451.
- T. Akyuz, A. Bassari, C. Bolcal, E. Sener, M. Yildiz, R. Kucer, Z. Kaplan, G. Dogan and S. Akyuz, Czech. J. Phys., 1999, 49(Suppl. 1, Pt. 1, 13th Radiochemical Conference, 1998),
- M. F. Araujo, A. Cruz, M. Humanes, M. T. Lopes, J. A. L. Da Silva and J. J. R. F. Da Silva, Chem. Speciation Bioavailability, 1999, 11(1), 25
- M. Y. Miah, M. K. Wang and M. Chino, J. Plant Nutr., 1999, 399 22(2), 229,
- M. Y. Miah and M. Chino, Bot. Bull. Acad. Sin., 1999, 40(2), 135.

- 401 S.-X. Bao, Z.-H. Wang and J.-S. Liu, Spectrochim. Acta, Part B, 1999, **54B**(13), 1893.
- 402 S. X. Bao and Z. H. Wang, Fenxi Huaxue, 1999, 27(5), 558.
- 403 D. Joseph, M. Lal, H. N. Bajpai and P. K. Mathur, J. Food Sci. Technol., 1999, 36(3), 264.
- 404 M. Harangozo, J. Tolgyessy, O. Tomecek, I. Ruzicka and K. Cejpek, J. Radioanal. Nucl. Chem., 1999, 240(3), 921.
- J. Ivanova, R. Djingova and I. Kuleff, J. Radioanal. Nucl. Chem., 1998, 238(1-2), 29.
- R. Djingova, J. Ivanova and I. Kuleff, J. Radioanal. Nucl. Chem., 1998, 237(1-2), 25.
- J. R. Bogert, H. J. Kwon, W. Jo, H. H. Kim, Y. W. Jeong, J. S. Lee, H. R. Yoon, I. S. Ban and C. H. Kim, Adv. X-Ray Anal., 1999, 41, 84.
- R. Kurt, W. Pitschke, A. Heinrich, H. Griessmann, J. Schumann and K. Wetzig, Proc. Int. Conf. Thermoelectr., 1998, 17th, 249.
- K. O. Goyal and J. W. Westphal, Adv. X-Ray Anal., 1998, 40, 1.
- J. Jurczyk, R. Sitko, B. Zawisza, F. Buhl and E. Malicka, 410 Mikrochim. Acta, 1999, **132**(1), 41.
- I. L. Eisgruber, T. L. Wangensteen, C. Marshall and B. Carpenter, *AIP Conf. Proc.*, 1999, 462(NCPV Photovoltaics 411 Program Review), 138.
- R. B. Kellogg, X-Ray Spectrom., 1999, 28(5), 406.
 A. D. Dane, H. A. van Sprang and L. M. C. Buydens, Anal. 413 Chem., 1999, 71(20), 4580.
- Y. Kataoka, N. Kawahara, T. Arai and M. Uda, Adv. X-Ray Anal., 1999, 41, 76.
- M. Mantler, Adv. X-Ray Anal., 1999, 41, 54.
- N. Ekinci, E. Baydas and Y. Sahin, Instrum. Sci. Technol., 1999, **27**(3), 181.
- P. Neumaier, JOT, J. Oberflaechentech., 1999(Spec., JOT Automotive Surface Technology), 84. V. Rossiger, *Metalloberflaeche*, 1999, **53**(4), 53.
- M. Klenk, O. Schenker, U. Probst and E. Bucher, Sol. Energy 419 Mater. Sol. Cells, 1999, 58(3), 299.
- M. Schulze, R. Reissner and M. Lorenz, Fresenius' J. Anal. Chem., 1999, 365(1-3), 178.
- M. F. Ebel, R. Svagera, M. Lindner, N. Praxmarer, C. Hager and 421 H. Ebel, Adv. X-Ray Anal., 1999, 41, 62. H. Ebel, R. Svagera, C. Hager, M. F. Ebel, C. Eisenmenger-
- Sittner, J. Wernisch and M. Mantler, Adv. X-Ray Anal., 1998, 40, 27
- 423 A. H. Ashour, M. B. S. Osman and S. M. Mokhtar, J. Polym. Mater., 1999, 16(1), 23.
- J. Jurczyk, R. Sitko, F. Buhl and I. Jendrzejewska, Chem. Anal. 424 (Warsaw), 1999, 44(2), 167.
- T. Konishi, J. Kawai, M. Fujiwara, T. Kurisaki, H. Wakita and Y. Gohshi, X-Ray Spectrom., 1999, 28(6), 470.
- M. Oku, K. Wagatsuma and T. Konishi, X-Ray Spectrom., 1999, 28(6), 464.
- S. Raj, H. C. Padhi and M. Polasik, Nucl. Instrum. Methods Phys. Res., Sect. B, 1999, 155(1-2), 143.
- S. Raj, H. C. Padhi, D. K. Basa, M. Polasik and F. Pawlowski, Nucl. Instrum. Methods Phys. Res., Sect. B, 1999, 152(4), 417.
- A. Kucukonder, E. Buyukkasap, R. Yilmaz and Y. Sahin, Acta Phys. Pol. A, 1999, 95(2), 243.
- U. Bergmann, C. R. Horne, T. J. Collins, J. M. Workman and
- S. P. Cramer, *Chem. Phys. Lett.*, 1999, **302**(1–2), 119. A. Yamaguchi, S. Hayakawa, K. Ono, H. Fujioka and M
- Oshima, Jpn. J. Appl. Phys., Part 1, 1999, 38(9A), 5077. D. F. Anagnostopoulos, R. Sharon, D. Gotta and M. Deutsch, Phys. Rev. A: At., Mol., Opt. Phys., 1999, 60(3), 2018.
- W. E. Wijsman and R. D. Vis, Nucl. Instrum. Methods Phys. Res., 433 Sect. B, 1999, **150**(1–4), 14.
- T. Mukoyama, B. Song and K. Taniguchi, X-Ray Spectrom., 1999, 28(2), 99.
- M. V. R. Murti, B. M. Rao, B. S. Reddy and K. Parthasaradhi, 435 Indian J. Phys. B., 1999, 73B(1), 93.
- I. Torok, T. Papp and S. Raman, Nucl. Instrum. Methods Phys. Res., Sect. B, 1999, 150(1-4), 8.
- S. N. Soni, Indian J. Phys. B., 1999, 73B(4), 661.
- S. N. Soni, J. Phys. B: At., Mol. Opt. Phys., 1999, 32(6), 1547.
- T. Yamamoto, A. Kanai, K. Hayashi and M. Uda, Nucl. Instrum. Methods Phys. Res., Sect. B, 1999, 150(1-4), 60.
- E. Baydas, O. Sogut, Y. Sahin and E. Buyukkasap, Radiat. Phys. Chem., 1999, 54(3), 217.
- J. T. Armstrong, Anal. Chem., 1999, 71(14), 2714.
- K. Lawniczak-Jablonska, J. Kachniarz, Z. Spolnik, J. Libera, E. Dynowska, A. Nadolny and J. Sadowski, J. Anal. At. Spectrom., 1999, 14(3), 461.

1441

- B. Song, H. Nakamatsu, A. Shigemi, T. Mukoyama and K. Taniguchi, *X-Ray Spectrom.*, 1999, 28(2), 94.
 J. Kawai, K. Hayashi, K. Okuda and A. Nisawa, *Rigaku Denki Janaru*, 1998, 29(1), 23.
- S. Latva, S. Peraniemi and M. Ahlgren, *Analyst (Cambridge, U. K.)*, 1999, **124**(7), 1105.
 A. van der Vegt and D. Norman, *Int. Lab.*, 1999, **29**(5A), 14.
 M. Harada and K. Sakurai, *Spectrochim. Acta, Part B*, 1999, **54**, 29.